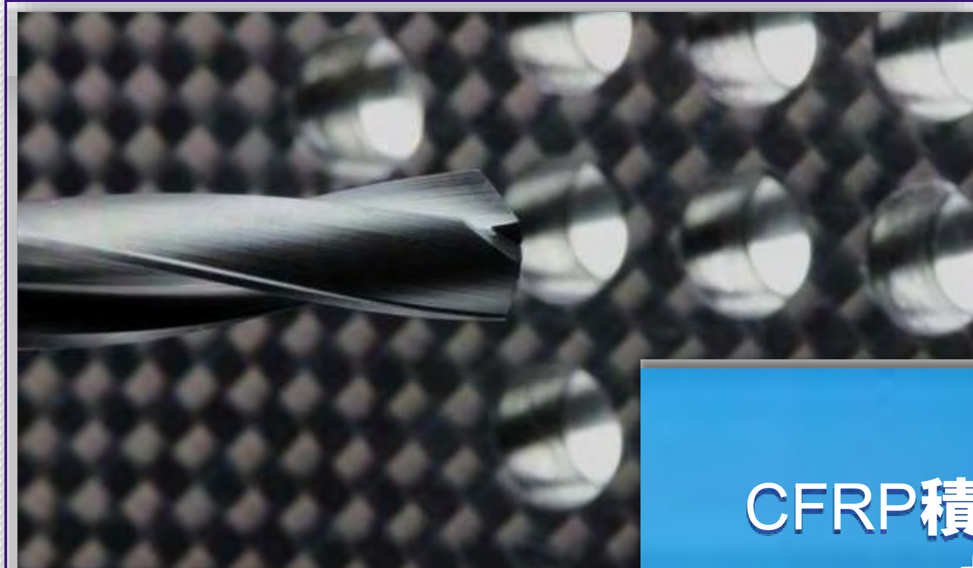

# CFRP積層板の穿孔損傷に関する実験および数値解析的研究


東北大学大学院 工学研究科 航空宇宙工学専攻

岡部朋永

TOHOKU UNIVERSITY

# 背景～適用が拡大する炭素繊維強化プラスチック

Boeing 787

- CFRP
- CFRPサンドイッチ
- GFRP
- アルミ合金
- 鋼・チタン　エンジンパイロン

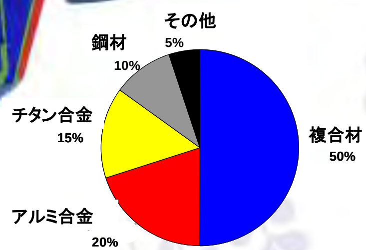


Airbus 350


MRJ

# Introduction

先行研究

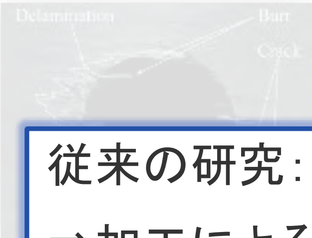


実験による加工条件と損傷に関する研究

従来の研究：穿孔後の損傷を主に評価

⇒加工による損傷が何を原因に発生・進展するかが未だ不明

数値解析による切削現象の研究

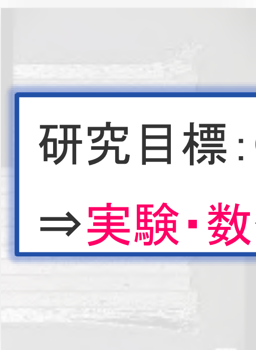

切削現象に着目

粒子法を用いた刃先先端の切削解析

刃先に生じる熱の解析

研究目標：CFRP積層板の穿孔損傷プロセス解明

⇒**実験・数値解析・理論解を併用した損傷プロセスの解明を実施**

# Experimental Study of Drilling Damage Initiation and Propagation

・貫通試験：3種類の送り速度にてスラスト荷重と穿孔損傷を観察する.

回転速度3240 rpm , 送り速度 $f$ = 120 , 230 , 375 mm/min (0.037 , 0.071 , 0.116 mm/rev)

使用ドリル:不二越 DCD10.0 (CFRP用ドリル，直径10 mm)

バックアッププレートの間隔$C$は，固定条件の影響を避けるため直径の5倍[3]とする



[3]N.Feito,J.Lopez-Puente,C.Satiuse,M.H.Migueluez,*Composite Structures* **108**(2014)677-683

# Experimental Study of Drilling Damage Initiation and Propagation

・貫通試験:3種類の送り速度にてスラスト荷重と穿孔損傷を観察する.

回転速度3240 rpm , 送り速度 $f$ = 120 , 230 , 375 mm/min (0.037 , 0.071 , 0.116 mm/rev)

使用ドリル:不二越 DCD10.0 (CFRP用ドリル, 直径10 mm)

バックアッププレートの間隔$C$は, 固定条件の影響を避けるため直径の5倍[3]とする

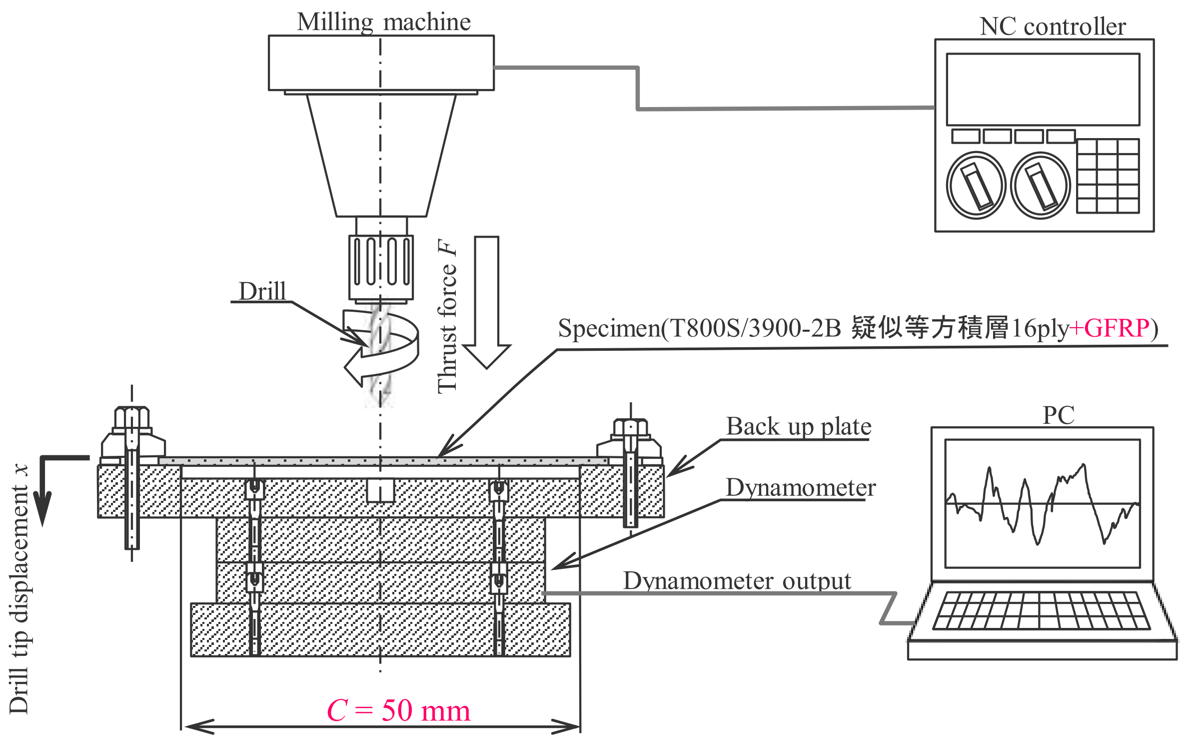


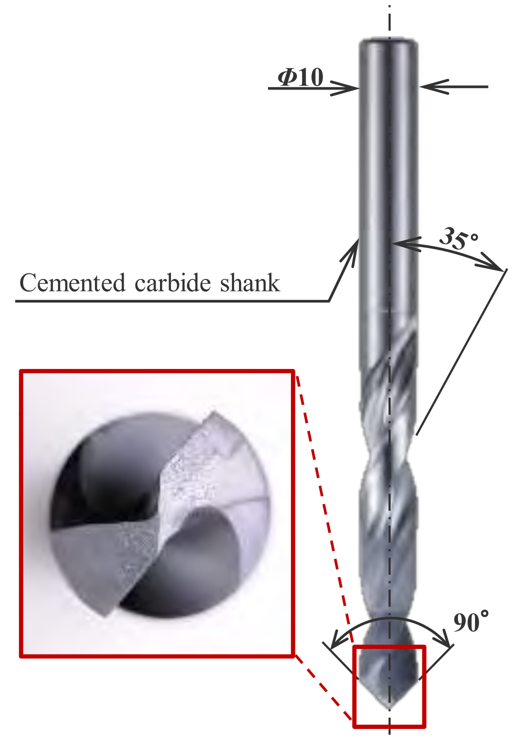



[3]N.Feito,J.Lopez-Puente,C.Satiuse,M.H.Migueluez,*Composite Structures* **108**(2014)677-683

# Experimental Study of Drilling Damage Initiation and Propagation

- 貫通試験結果

スラスト荷重履歴は送り速度に対し相似関係

最大スラスト力$F_{max}$は送り速度に対し線形に増加

損傷規模(はく離面積)は送り速度に対し線形に増加

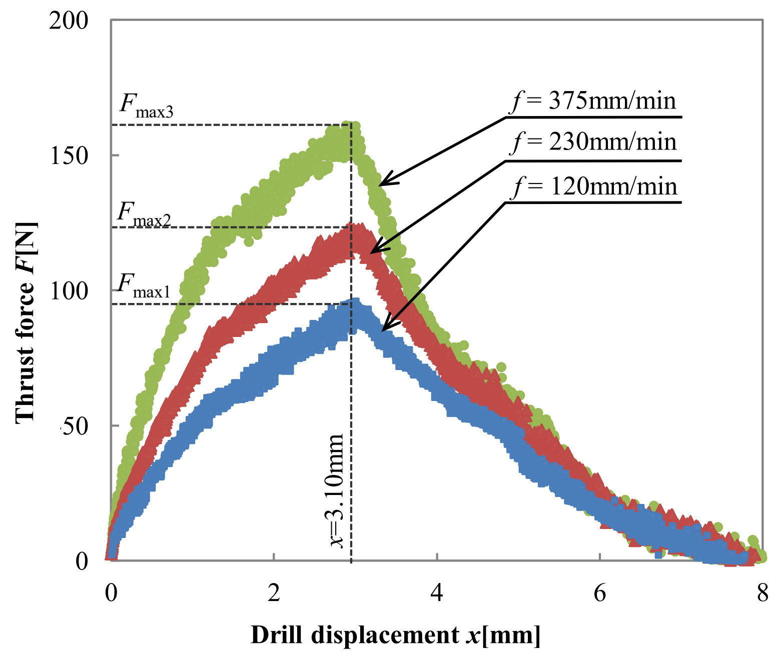


各送り速度におけるスラスト荷重履歴

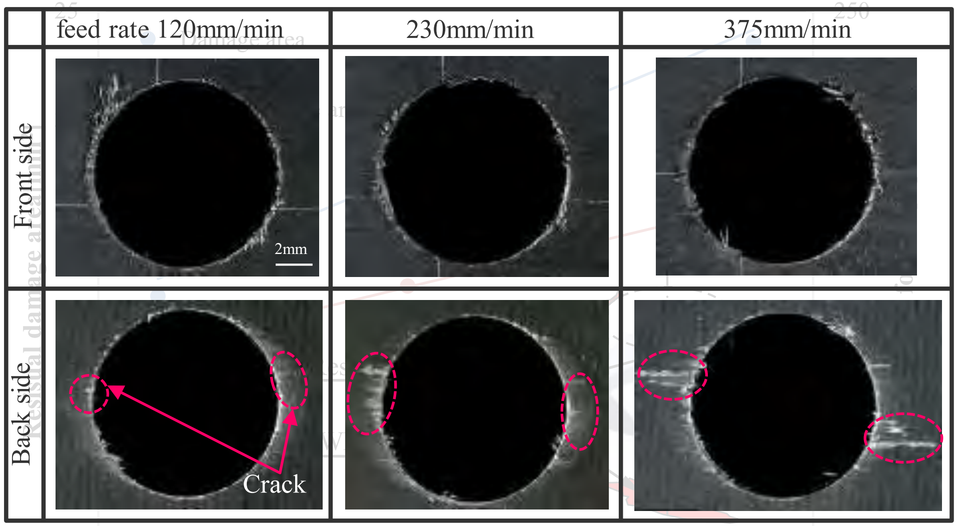


各送り速度における穿孔の表裏観察結果

送り速度に対する損傷面積および最大スラスト力の応答

- 結論：送り速度に対しスラスト荷重および損傷規模は線形関係である

⇒適用した加工条件下では損傷プロセスは同一であると思われる

# Experimental Study of Drilling Damage Initiation and Propagation

- 貫通試験結果

  スラスト荷重履歴は送り速度に対し相似関係

  最大スラスト力$F_{max}$は送り速度に対し線形に増加

  損傷規模(はく離面積)は送り速度に対し線形に増加

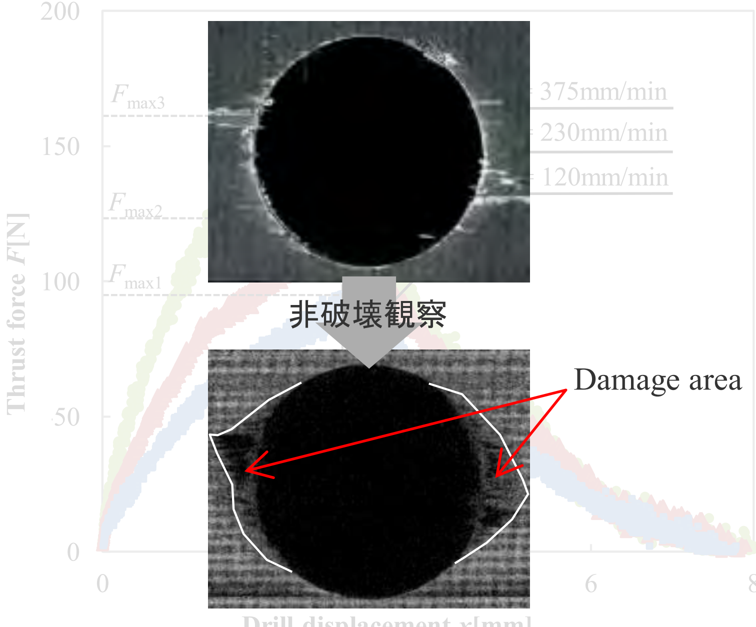


各送り速度におけるスラスト荷重履歴

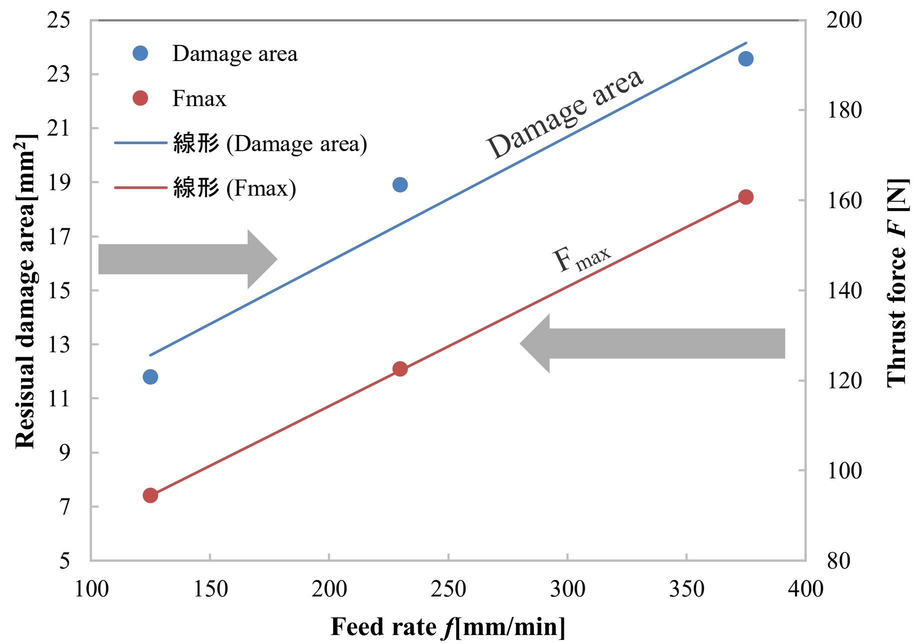


送り速度に対する損傷面積および最大スラスト力の応答

- 結論：送り速度に対しスラスト荷重および損傷規模は線形関係である

  ⇒適用した加工条件下では損傷プロセスは同一であると思われる

# Experimental Study of Drilling Damage Initiation and Propagation

・途中止め試験の条件

貫通試験を参考にA-Cの計3点で非破壊検査，送り速度 $f$ = 375 mm/min,回転数 3240 rpm

・結果

損傷は最大スラスト力が生じた後に発生し，穿孔完了間際までGFRPの一部が残留する

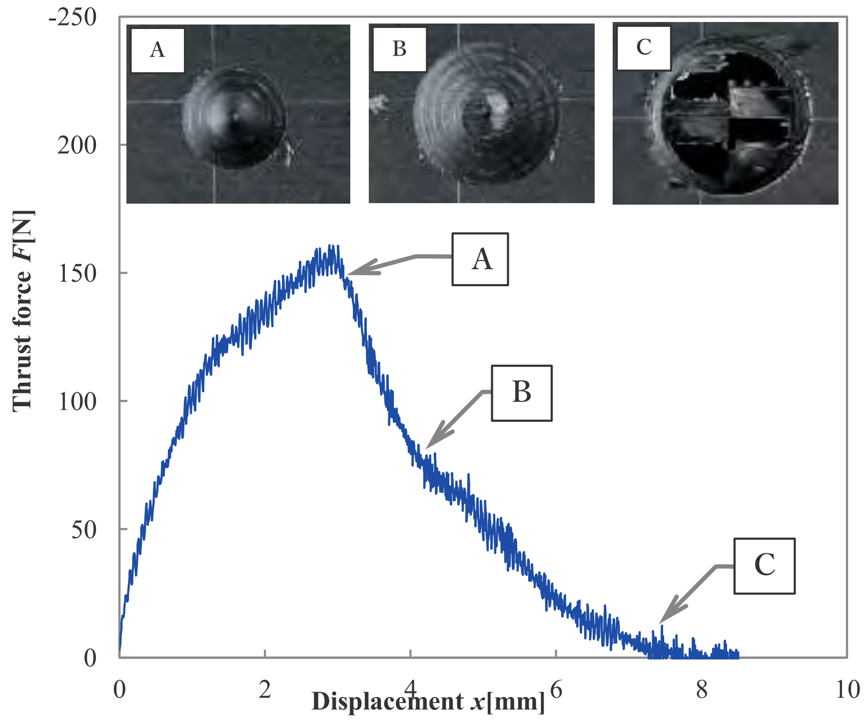

途中止め試験から得られた15Ply-16ply間の非破壊検査結果

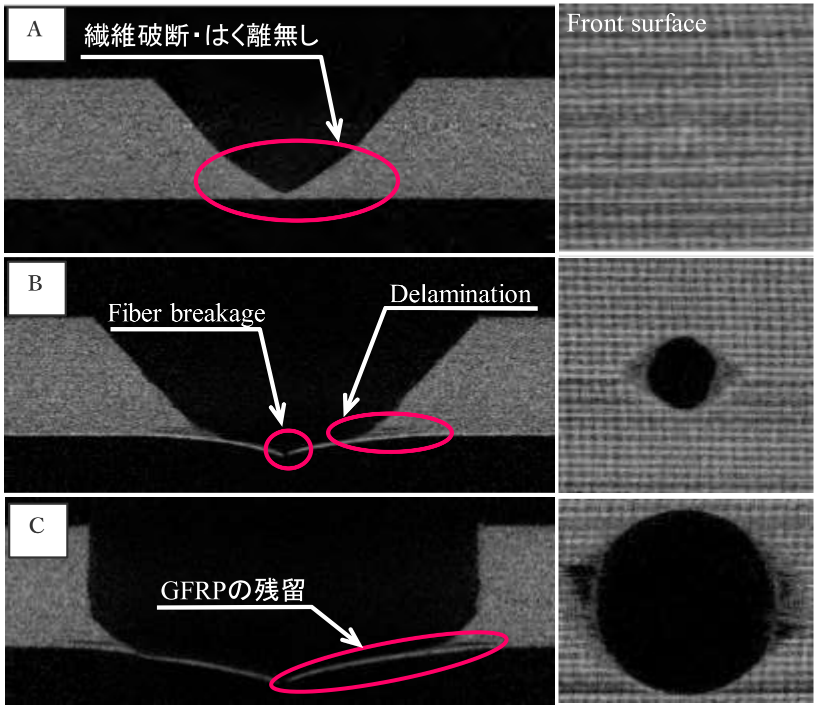

非破壊検査における断面写真

・結論：GFRP+第16層の一部が残留+押出を受けて損傷が進展する

東北大学

# Experimental Study of Drilling Damage Initiation and Propagation

・結果II

A→BのタイミングでGFRP層を貫通する十字型のクラックが生じる

⇒十字型のクラックに伴い層間はく離が発生する.

⇒十字型のクラック＝第16層のCFRPのトランスバースクラック＋GFRPの繊維破断

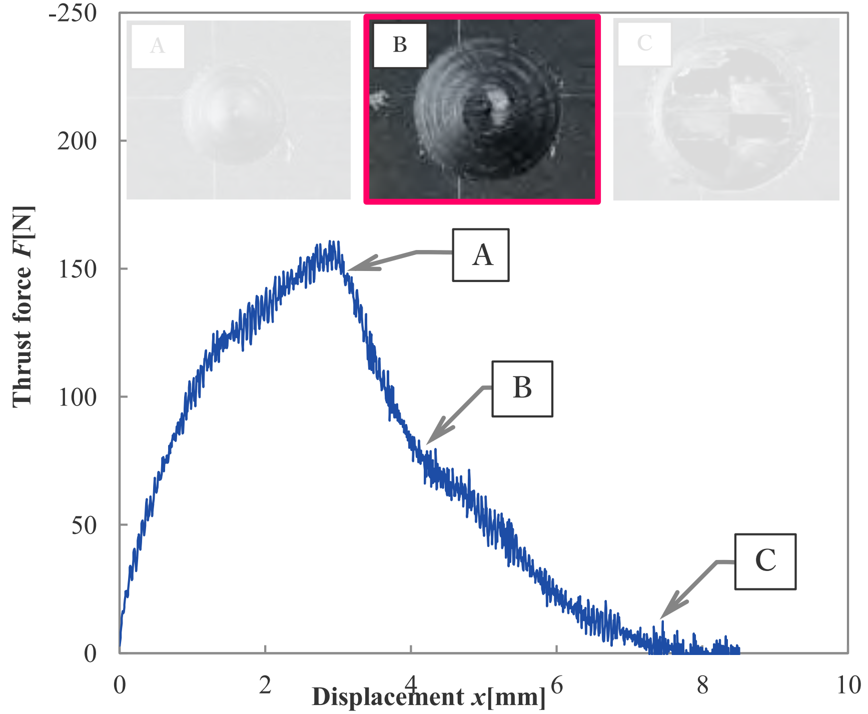


途中止め試験から得られた15Ply-16ply間の非破壊検査結果

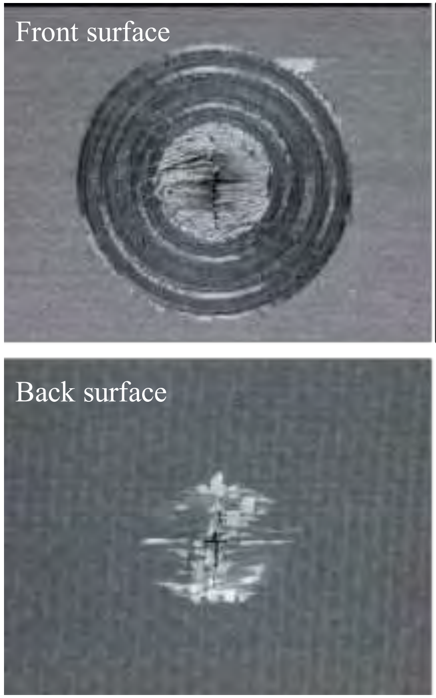


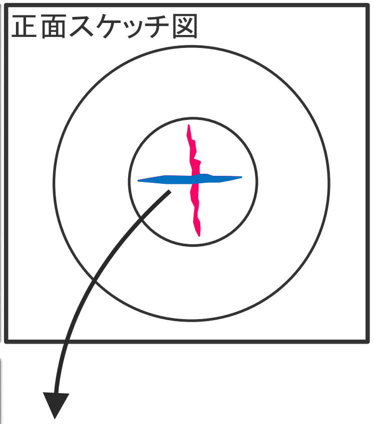


赤色のクラック
⇒GFRPの繊維破断
青色のクラック
⇒第16層トランスバースクラック
＋GFRPの繊維破断

途中止め試験から得られた十字型クラックの観察結果

⇒実験から観察された損傷を導入した数値解析で，損傷挙動を詳細に検証する

# Numerical Modeling for Drilling Damage

・CFRPに生じる損傷現象とそのモデル化

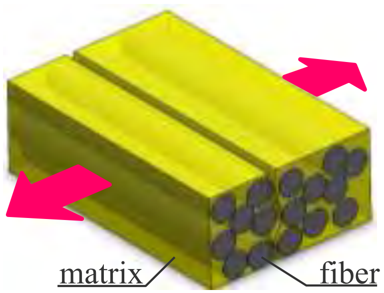


繊維間のマトリクスクラック：Continuum Damage Mechanics(CDM)[4]

・Helmholtz自由エネルギーを介し，変形と損傷の関係を算出

・要素の変形量から，その要素の剛性を決定する

繊維破壊:Smeared Crack Model(SCM)[5]

・繊維破壊に伴う解放エネルギーを考慮し，要素のσ-ε関係を算出

・要素の変形量から，その要素の剛性を決定する

生じた損傷(マイクロクラック・繊維破断)による剛性低下

界面の結合・分離挙動

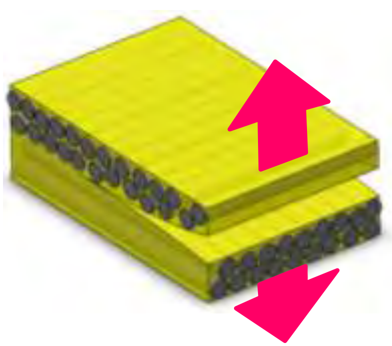

層間はく離:Cohesive zone model(CZM)

・応力基準を満たした時点から界面の分離を開始

・開口に伴う解放エネルギーから界面の結合力を算出




[4]A.Yoshimura et al,ASC2012
[5]S.T.Pinho et al, *Composites PartA*, 2006

# Fracture process of laminate

## Typical damages seen in composite laminates

The multiple damages are generated in composite laminates under the applied load.

① Transverse cracks
(Cracks in a direction parallel to the fiber)

② Delamination

③ Fiber breakage

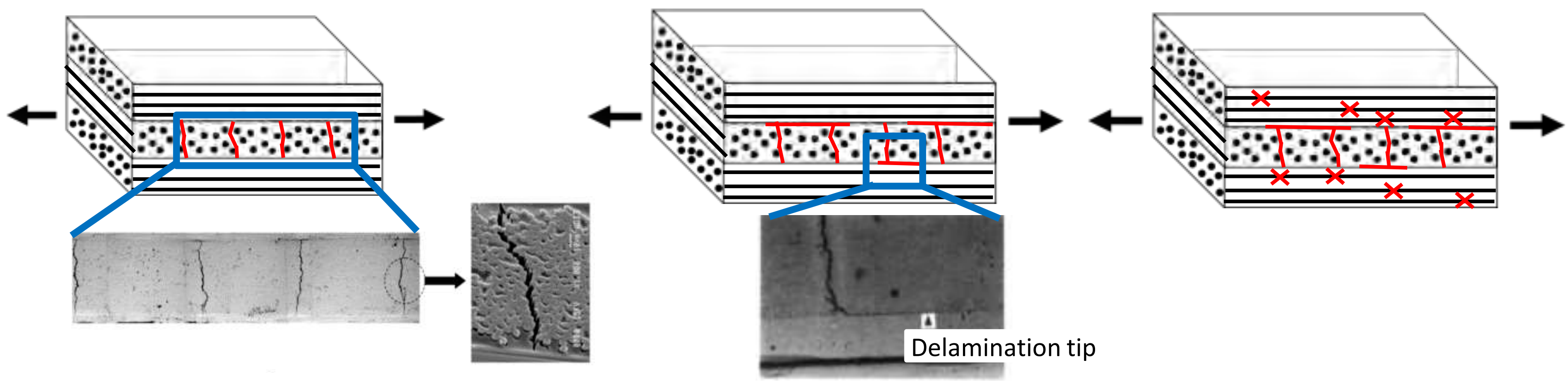


First, the transverse cracks occur at the lower strain. Secondly, the delamination will be induced by the cracks. Finally, the composites will fail due to the multiple fiber breaks.

# Two types of damage modelling for composite laminates

For the modelling of cracks in standard FEM, two approaches have been widely used .

| | Continuous modelling (CM) approach | Discrete modelling (DM) approach |
|---|---|---|
| Model | Smeared crack model (SCM)<br>Continuum damage mechanics (CDM) | Cohesive interface element<br>Spring element |
| Overview | The damage is modelled through the constitutive relation. The crack is expressed as the band having the element thickness<br>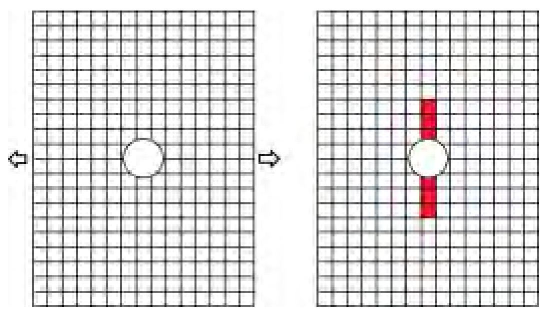 | Zero thickness elements are inserted at crack location to model the interface connection and separation.<br>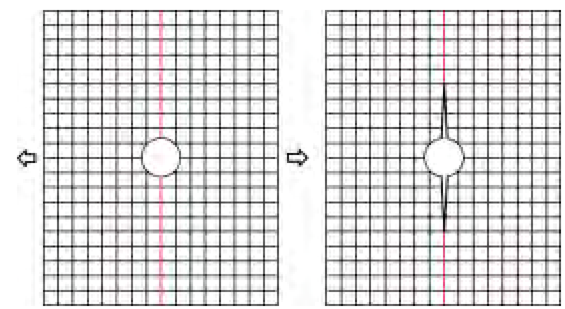 |
| Advantage | Computational robustness<br>Ability to model the unknown location cracks | Ability to capture stress concentration around the crack tip |
| Disadvantage | Lack of ability to capture stress concentration around crack tip. | Application is limited for the problem where crack locations are known. |
| Application | ○ Multiple (Diffuse) Crack<br>× Large (Dominant) Crack | ○ Large (Dominant) Crack<br>× Multiple (Diffuse) Crack |

# Topics of this presentation

This presentation introduces our recent studies based on the continuum damage mechanics.

(1) Progressive failure modeling of Open Hole Tension of quasi-isotropic laminates

R. Higuchi, T. Okabe, T. Nagashima, "Numerical simulation of progressive damage and failure in composite laminates using XFEM/CZM coupled approach", Composites Part A: Applied Science and Manufacturing 95(2017), 197-207

(2) Numerical simulation for the High velocity impact

R. Higuchi, T. Okabe, A. Yoshimura, T. E. Tay, "Progressive Failure under High-Velocity Impact on Composite Laminates; Experiment and Phenomenological Mesomodeling", Engineering Fracture Mechanics 178 (2017), 346-361.

(3) Analytical derivation of the relationship between damage tensor and multiple cracks

Tomonaga Okabe, Sota Onodera, Yuta Kumagai and Yoshiko Nagumo, "Continuum damage mechanics modeling of composite laminates including transverse cracks", International Journal of Damage Mechanics, accepted

# Open-Hole Tensile (OHT) Test

## Open-Hole Tensile (OHT) Test

Practical strength assessment method.
⇒Strength depends on specimen size, so that a variety of specimens are needed.
⇒**<u>Taking all types of strength data by only experiment is time-consuming and inefficient.</u>**


Failure modes on CFRP laminate.

Therefore, the numerical simulation procedure should be established to predict the progressive failure process instead of experiments

## Numerical simulation for CFRP OH laminate

- Fiber breakage ……**Weibull Criterion**
- Matrix crack, Delamination……**Cohesive Element Model**

⇒**They could successfully reproduce the failure mode transition .**
⇒**Cohesive element requires high computational cost.**

(S. R. Hallett et al., *Compos. Part A*, 2009)

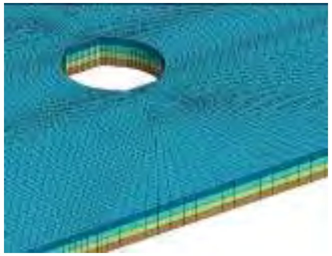

FE simulation mesh for CFRP laminate OHT

**We presented the progressive failure simulation of OHT with a hybrid model (CM plus DM).**

# Experiments

**<u>OHT experiment</u>** (B. G. Green et al., *Compos. Part A*, 2007)

- OHT tests on IM7/8552 laminates by Green et al.
- Laminate properties : $[45°/90°/-45°/0°]_S$
- Failure mode depends on thickness of specimen.

⇒Failure modes : 1mm (**Brittle**) and 2, 4, 8mm (**Delamination**)

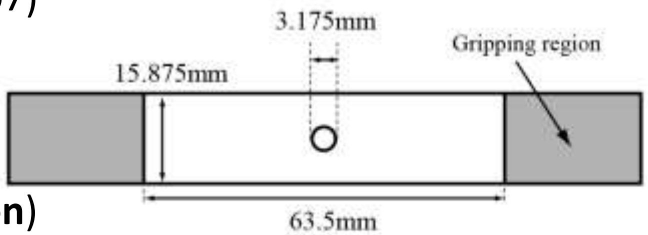


Specimen dimension

**FE simulation should reproduce the change of failure modes automatically.**

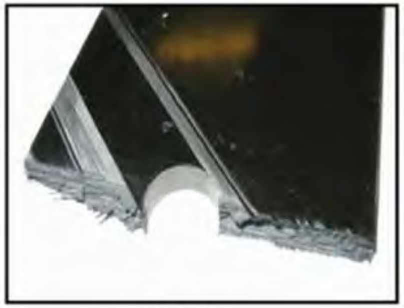

Brittle

**Fiber breakage** driven failure

Delamination

**Delamination** driven failure

# Three types of failure model or method on the damage progress

## Weibull criterion

This assumes the weak-link scaling based on Weibull distribution as like brittle materials.

・More than 1 vulnerable point in an element volume determines ultimate failure.

## Cohesive element (CE)

The zero thickness elements represent interface cohesion.

Pros : Capability of capturing stress concentration at the crack tip.

Cons : Small element size and high computational cost.

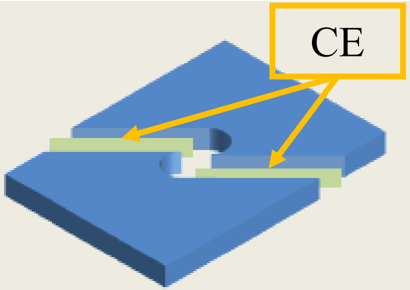


## Continuum damage mechanics (CDM) (A. Yoshimura et al., ASC 2012)

Implement damage effect caused by micro cracks in continuum body into constitutive tensor.

Pros : Capability  of representing unknown crack position.

Cons : Crack width relying on element size.

# Numerical models on damage progress

| Model (i) | Model(ii) | Model (iii) |
|---|---|---|
| All plies : **CDM** | 0° ply : CE, Others : **CDM** | All plies : CE |
| 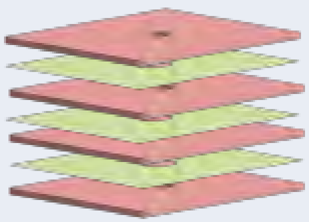 45° ply<br>45°/90° interface<br>90° ply<br>90°/-45° interface<br>-45° ply<br>-45 °/0° interface<br>0° ply | 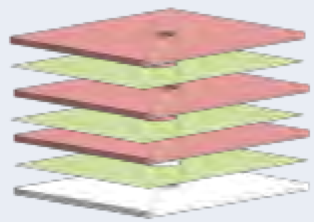 45° ply<br>45°/90° interface<br>90° ply<br>90°/-45° interface<br>-45° ply<br>-45 °/0° interface<br>0° ply | 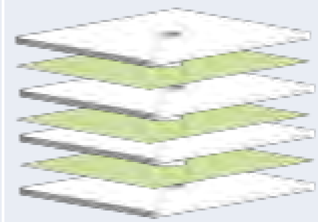 45° ply<br>45°/90° interface<br>90° ply<br>90°/-45° interface<br>-45° ply<br>-45 °/0° interface<br>0° ply |
| 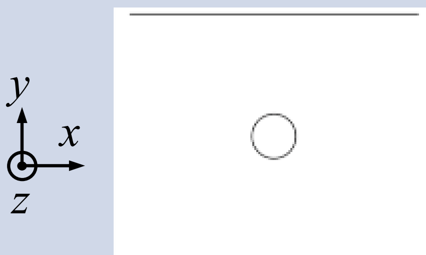 y<br>x<br>z | 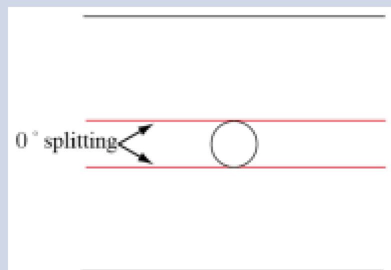 0° splitting | 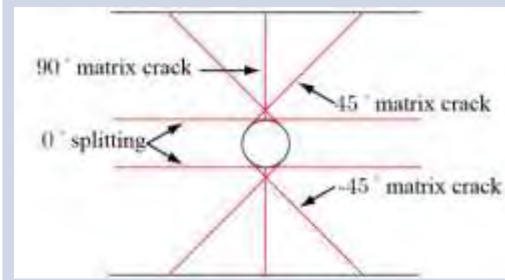 90° matrix crack<br>45° matrix crack<br>0° splitting<br>-45° matrix crack |
| 56752 nodes | 60552 nodes | 173856 nodes |

- All models used Weibull criterion for FB and Cohesive element for delamination.
- Modellings of in-plane matrix cracks are different.

# Schematic figure of simulation model

**<u>Simulation model</u>**

・Boundary conditions are shown in the figure.

・Minimum element size was determined by cohesive zone length (CZL)[5)].

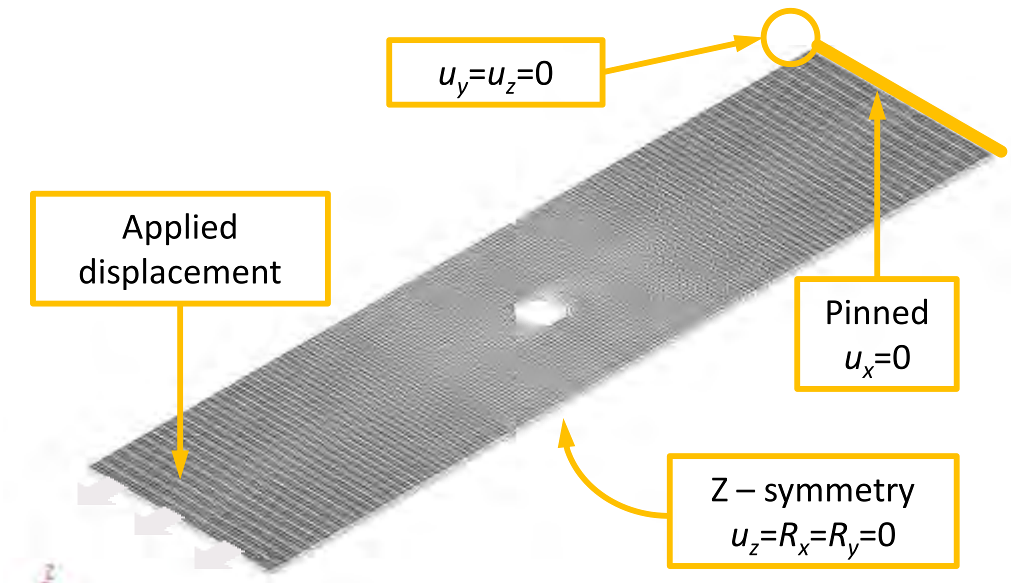


Computational model and boundary conditions. (Model (iv))

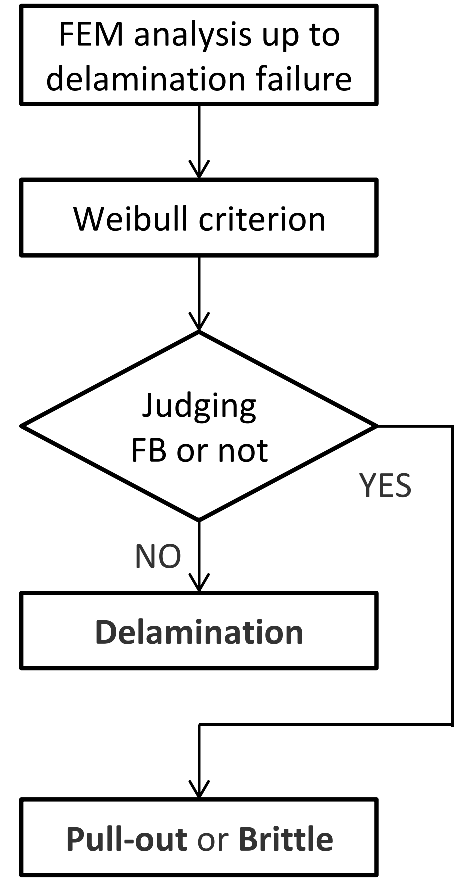


Failure mode determination flow

# Simulation results with experiments

## Computational result

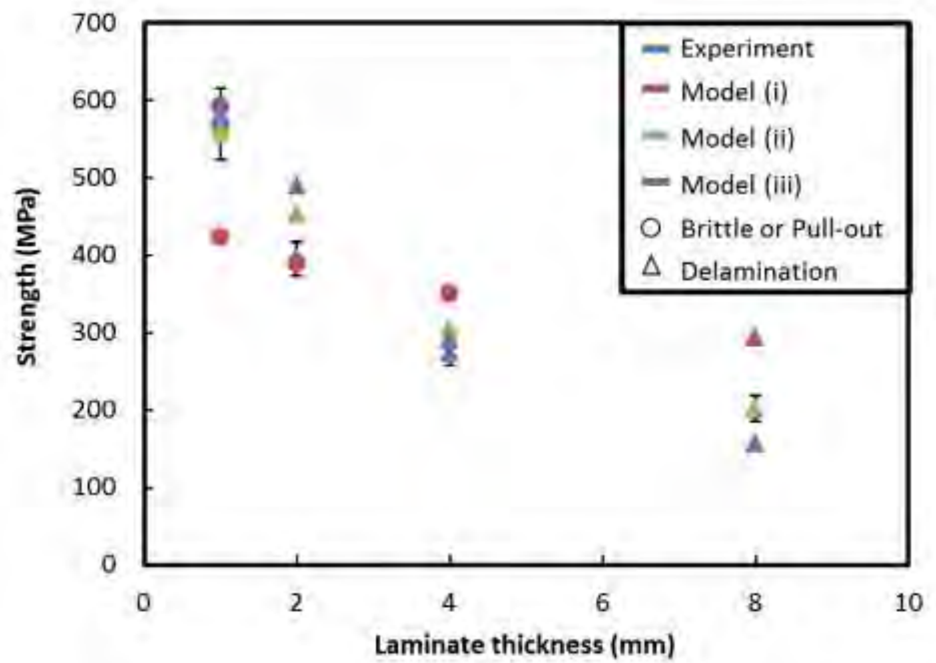


Relationship of strength and lainate thickness

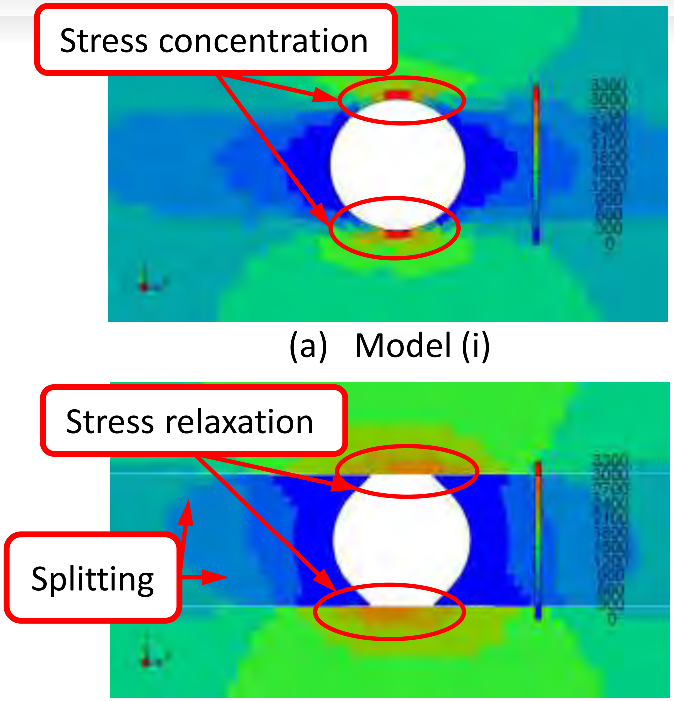


(a) Model (i)

(b) Model (ii)

X stress distribution on 0 degree ply around hole

- Model (ii), (iii) can estimate all of the strength and failure modes.
- However, Model (i) cannot estimate failure mode.

⇒CDM can't capture stress relaxation caused by splitting in 0° ply.

⇒ DM modeling of splitting is VERY important for strength estimation.

⇒The computational cost of Model (iii) is the highest, similar to Hallet et al.

**The hybrid approach is the most appropriate and effective for modeling of OHT.**

# High−velocity impact

## Background

- **The application of CFRP to the aircraft engine fan-system (Fan blades, Fan cases) has been increased.**
- **The risk of high-velocity impacts is significant.**
  ex) Bird-strikes, Impacts of broken fan blade
- **Full-scale experimental tests are expensive and time consuming .**

**We tried to develop the efficient numerical simulation tools for high-velocity impact**

**Objective**

## Recent works

Raimondo et al. (2007), *ICCM 16th*

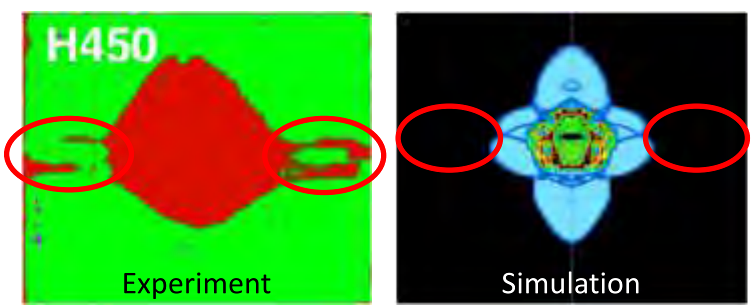


Yoshimura et al. (2012), *ASC 27th*

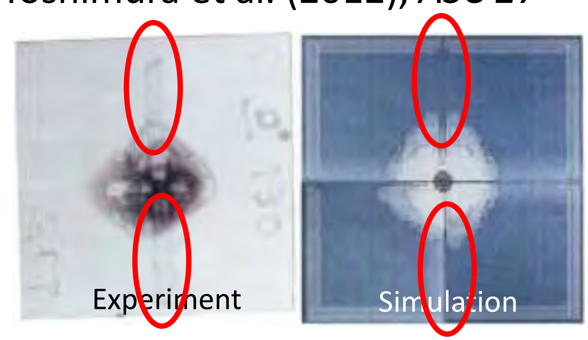


Both simulation could not predict large transverse cracks in the bottom ply, because they used only the CM.

# This presentation

**Experiments of high velocity impacts**
**→Information for numerical modelling**

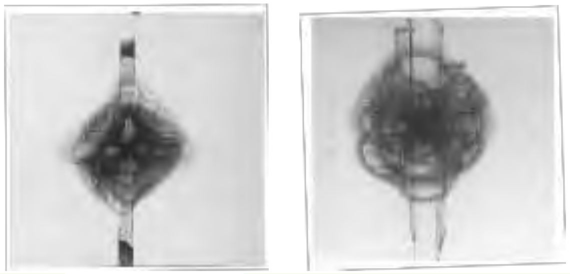

**Experiment**

**Simulation**

**Objective**

**To develop the efficient numerical simulation tools for high-velocity impact**

Three types of numerical simulations for the comparison.

**(i) Hybrid simulation model**

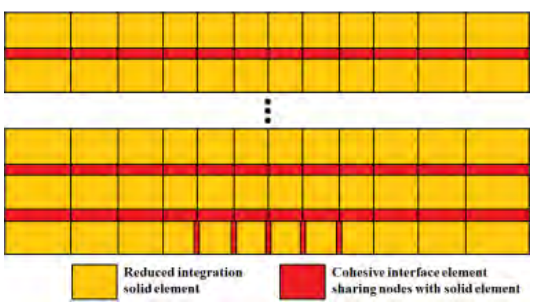


vs.

**(ii) Discrete simulation model**

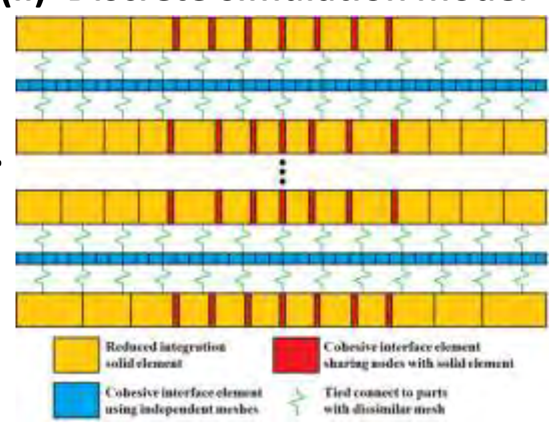


vs.

**(iii) Continuous damage model**

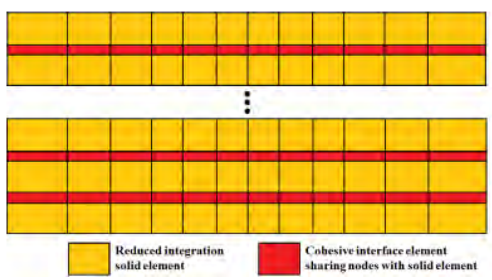

# Testing Procedure

## High-Velocity Impact Test

Single-stage air gun was used for high-velocity impact test.

Specimen : T700S/#2592(Toray), $[0/90]_{4S}$, (L) 60mm × (W) 60mm × (T) 1.9mm

Projectile : $\phi = 6.0\text{mm}$, weight = 0.9g

Sabot : Expanded polystyrene

Impact velocity : $120 - 130\ (\text{m/s})\ (Range\ of\ no\ penetration)$,

$180 - 200\ (\text{m/s})\ (Range\ of\ penetration)$

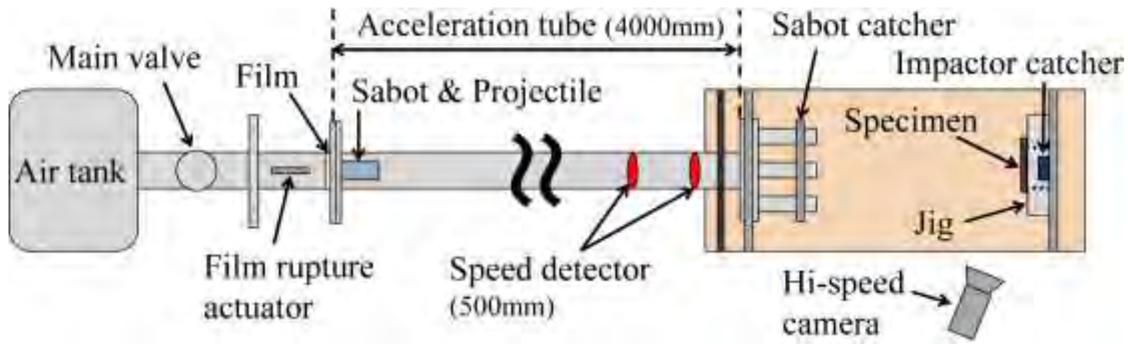



## Nondestructive Inspection (NDI)

•Soft X-ray microfocus CT (TOSCANER-30000μhd, TOSHIBA IT & Control Systems Corp.)

Sectional images, Three-dimensional images

•Soft X-ray radiograph (SV-100AW, SOFTEX, Inc.)

# Experiment

No Penetration Case

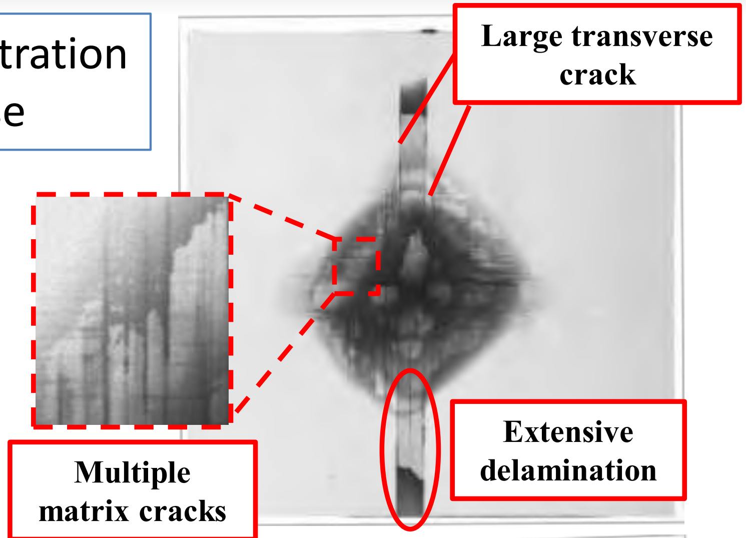


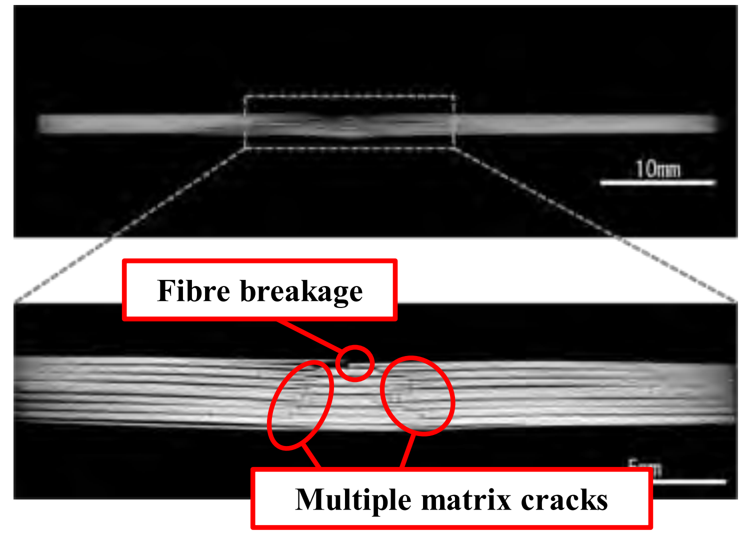


Penetration Case

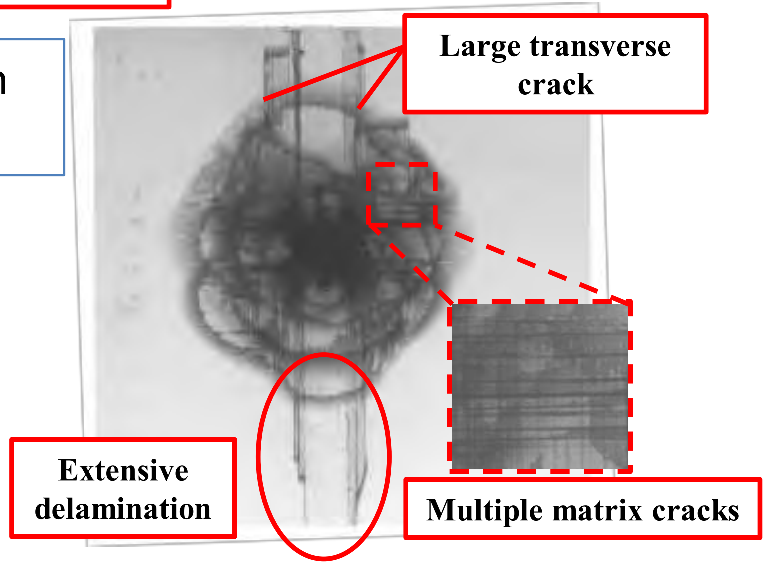


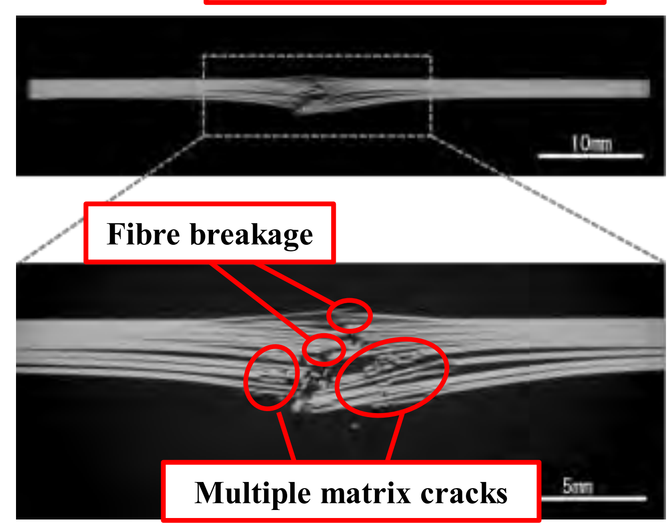

# Experiment

Internal damage distributions

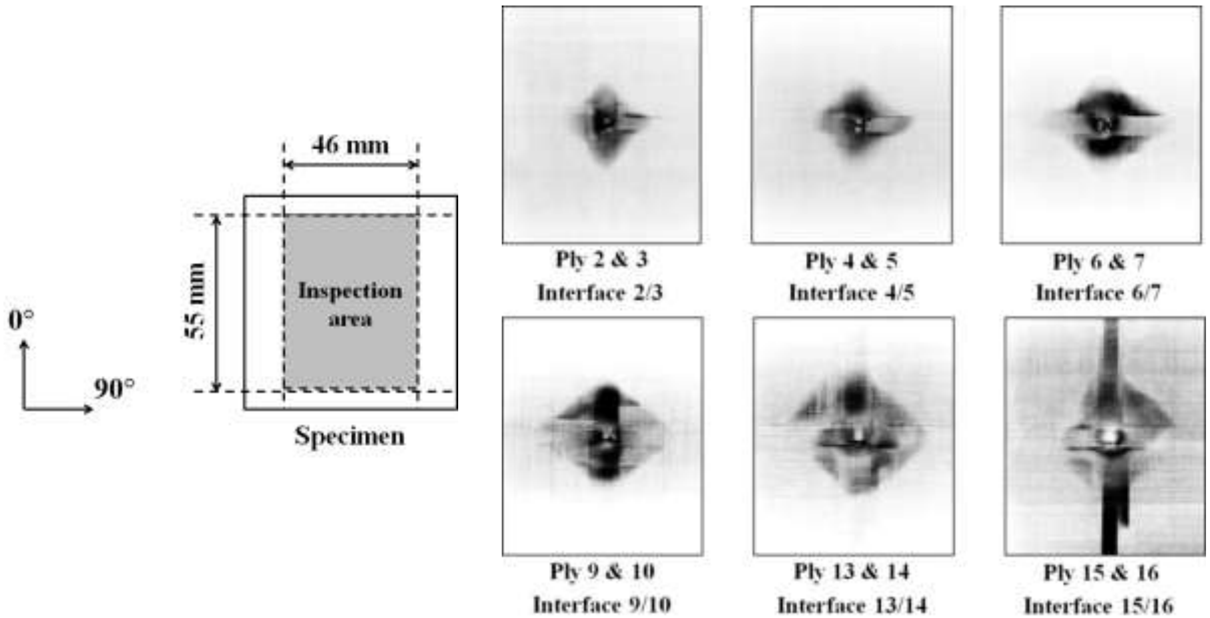


Greater degree of damage occurred at the lower plies and interfaces

The shape of delaminations was determined by two major matrix cracks

Findings from experimental observations

- **Three damage mechanisms** were primarily observed: fibre breakage, matrix crack, and delamination.
- Observed matrix cracks can be classified into two categories: **multiple matrix cracks** occurring around the impact point and **large transverse cracks** on the bottom ply.
- The shape of delaminations was determined by **two major matrix cracks**.

# Simulation model for damage progression on the HVI

We did three types of numerical simulations for the comparison.

Model (I)

Fibre breakage → Smeared Crack Model (SCM)
Delamination → Cohesive interface element
Matrix cracks → Continuum Damage Mechanics (CDM) model + Cohesive interface element

**Except for bottom ply : CDM model**
**Bottom ply : Cohesive interface element**

} **Hybrid model**

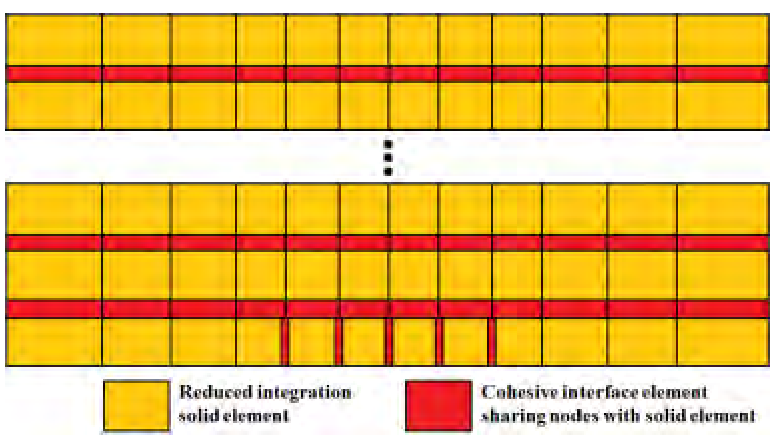


Model setups

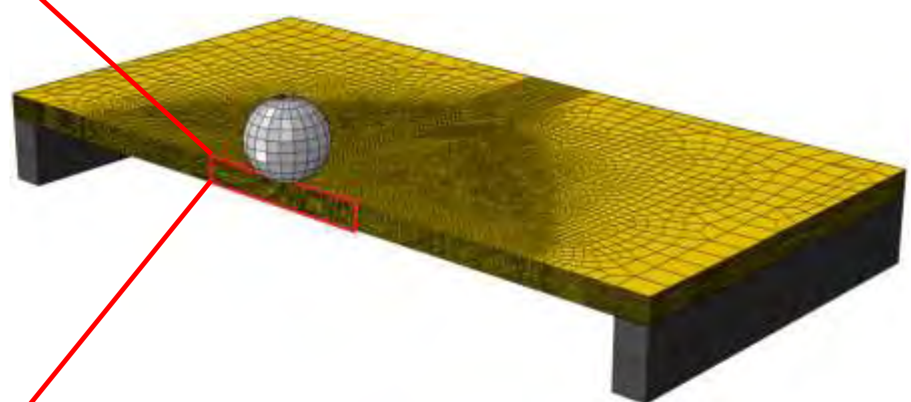

Simulation model

# Simulation model

Model (II)

Fibre breakage → Smeared Crack Model (SCM)
Delamination → Cohesive interface element
Matrix cracks → Cohesive interface element

**All plies : Cohesive interface element** →Model (ii) is a typical DM approach.

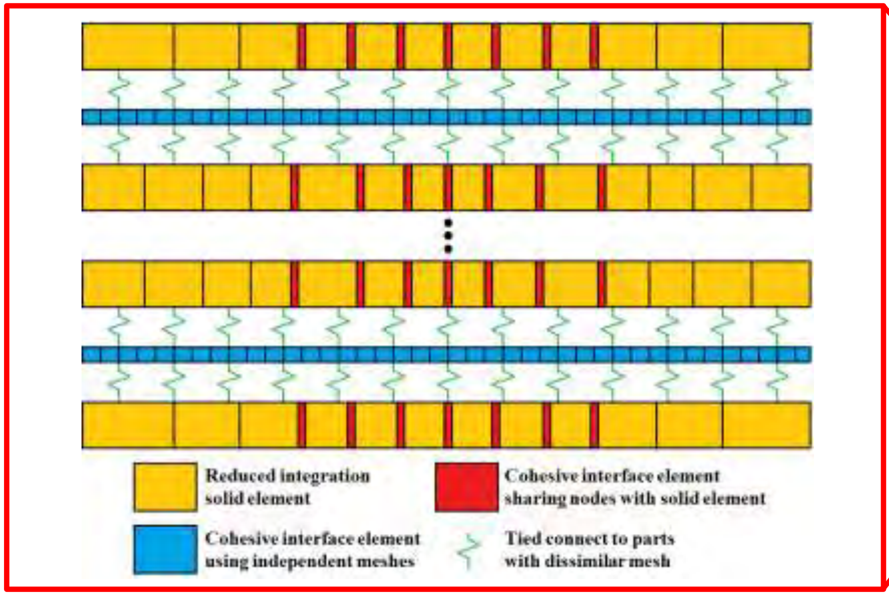


Model setups

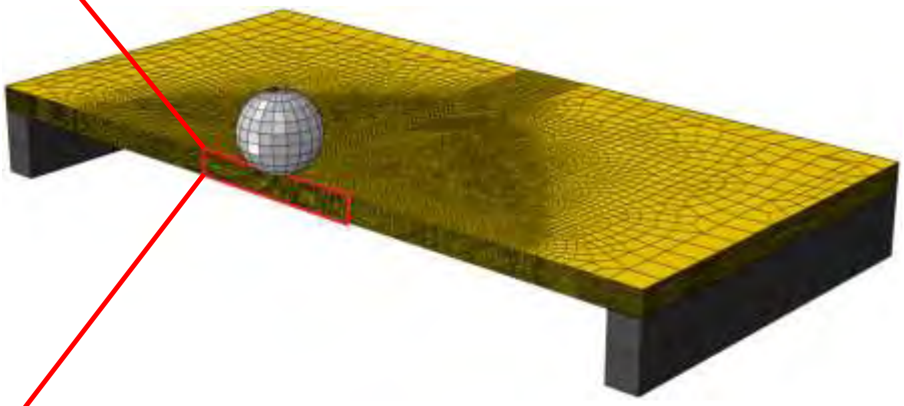

Simulation model

# Simulation model

## Model (III)

Fibre breakage → Smeared Crack Model (SCM)
Delamination → Cohesive interface element
Matrix cracks → Continuum Damage Mechanics (CDM) model

**All plies : Continuum damage mechanics (CDM) model** →Model (III) is a typical CM approach.

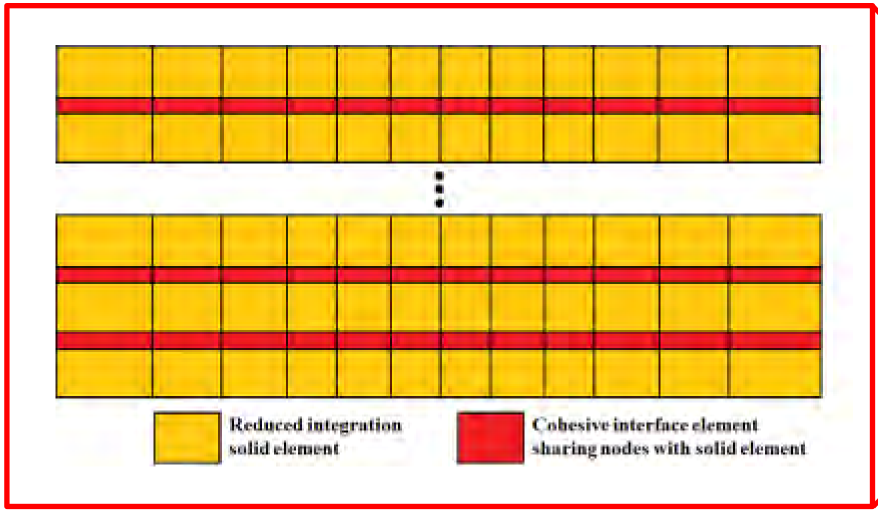


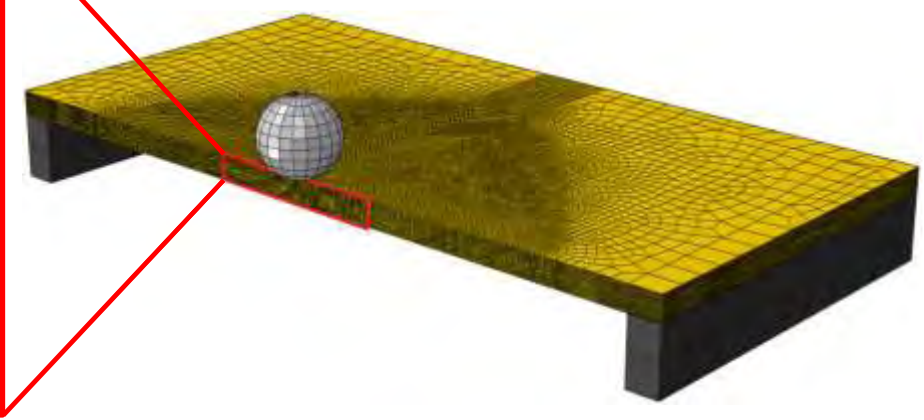

Model setups

Simulation model

# Details of numerical simulation

## Simulation models and boundary conditions

- High-velocity impact simulations were performed using **Abaqus/Explicit.**
- Each damage models were implemented through user-written subroutine **VUMAT**.
- '**General contact algorithm**' was used for contact between the projectile and the laminate and that between the jig and the laminate

## Element Removing Criteria

(Raimondo et al. (2007), *ICCM 16th* )

To prevent excessive distortion of the elements, the following criteria were implemented.

(i) Damage variables based criteria

$$f^{\mathrm{d}}_{\mathrm{removing}} = \min\left(d^{\mathrm{T}}_{1\mathrm{C}} - d^{\mathrm{T}}_{1}, d^{\mathrm{C}}_{1\mathrm{C}} - d^{\mathrm{C}}_{1}\right) = 0$$

$$\text{with}: \quad d^{\mathrm{T}}_{1\mathrm{C}} = 0.999, d^{\mathrm{C}}_{1\mathrm{C}} = 0.99$$

(ii) Strain components based criteria

$$f^{\mathrm{s}}_{\mathrm{removing}} = \min\left\{\varepsilon_{\mathrm{C}} - \max\left(\varepsilon_{11}, \varepsilon_{22}, \varepsilon_{33}\right), \gamma_{\mathrm{C}} - \max\left(\gamma_{12}, \gamma_{23}, \gamma_{31}\right)\right\} = 0$$

$$\text{with}: \quad \varepsilon_{\mathrm{C}} = 0.4, \ \gamma_{\mathrm{C}} = 1.25$$

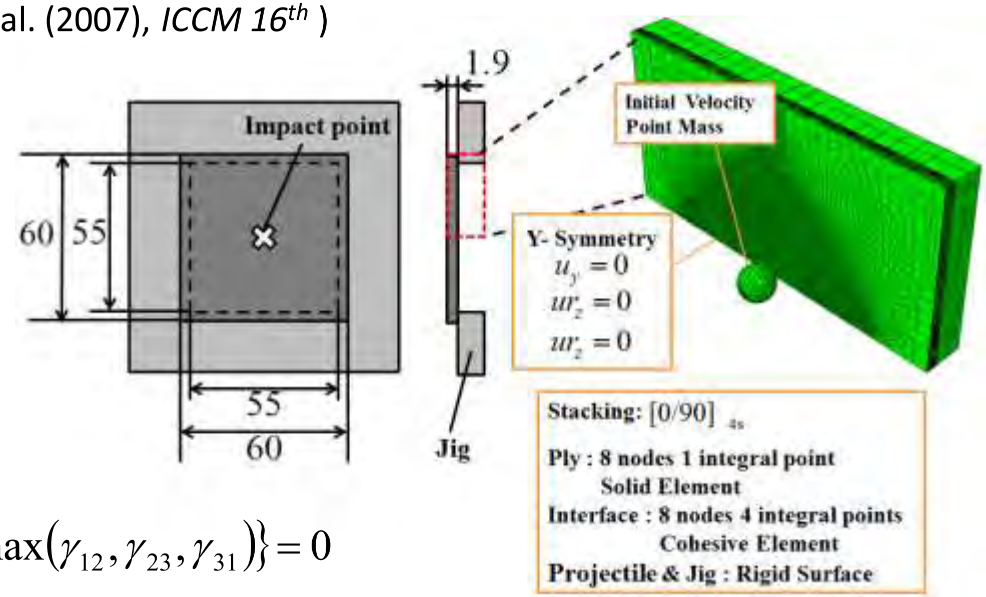

# Animation of impact behaviors in this simulation

(a) No Penetration Case
Model(I) @120m/s

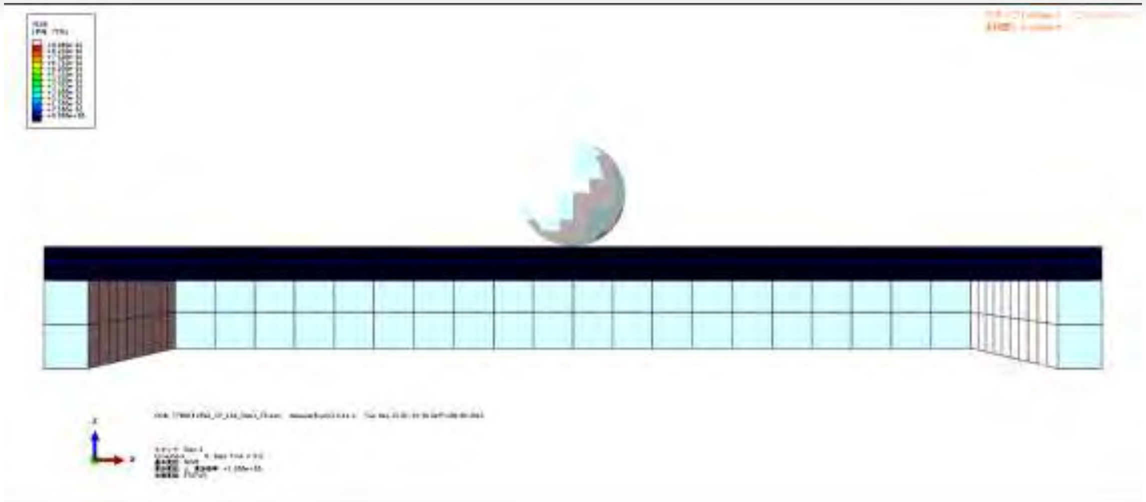

(b) Penetration Case
Model(I) @180m/s

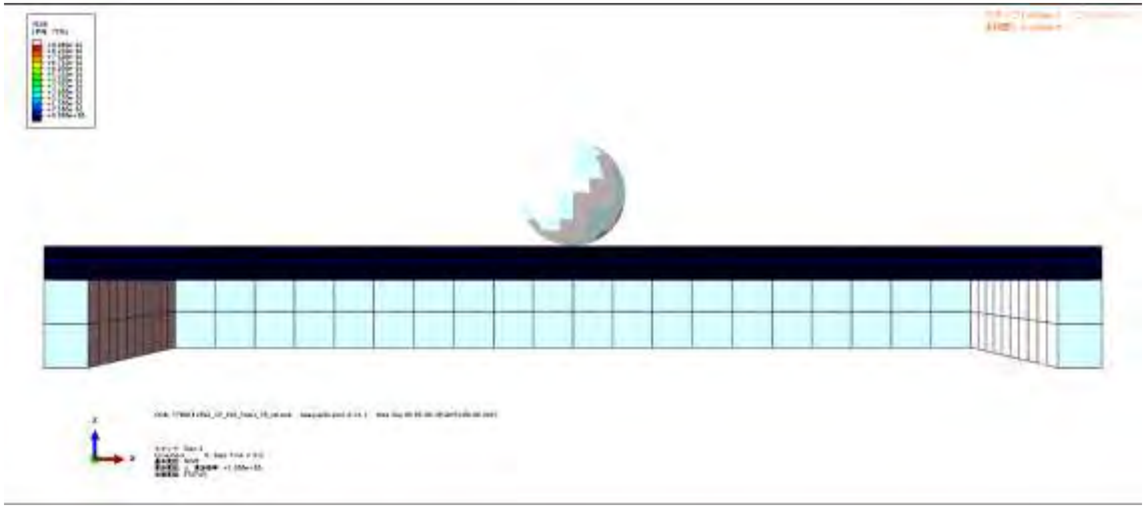

The proposed simulation could reproduce the transition from no-penetration to penetration successfully.

# Comparison between experiments and simulations

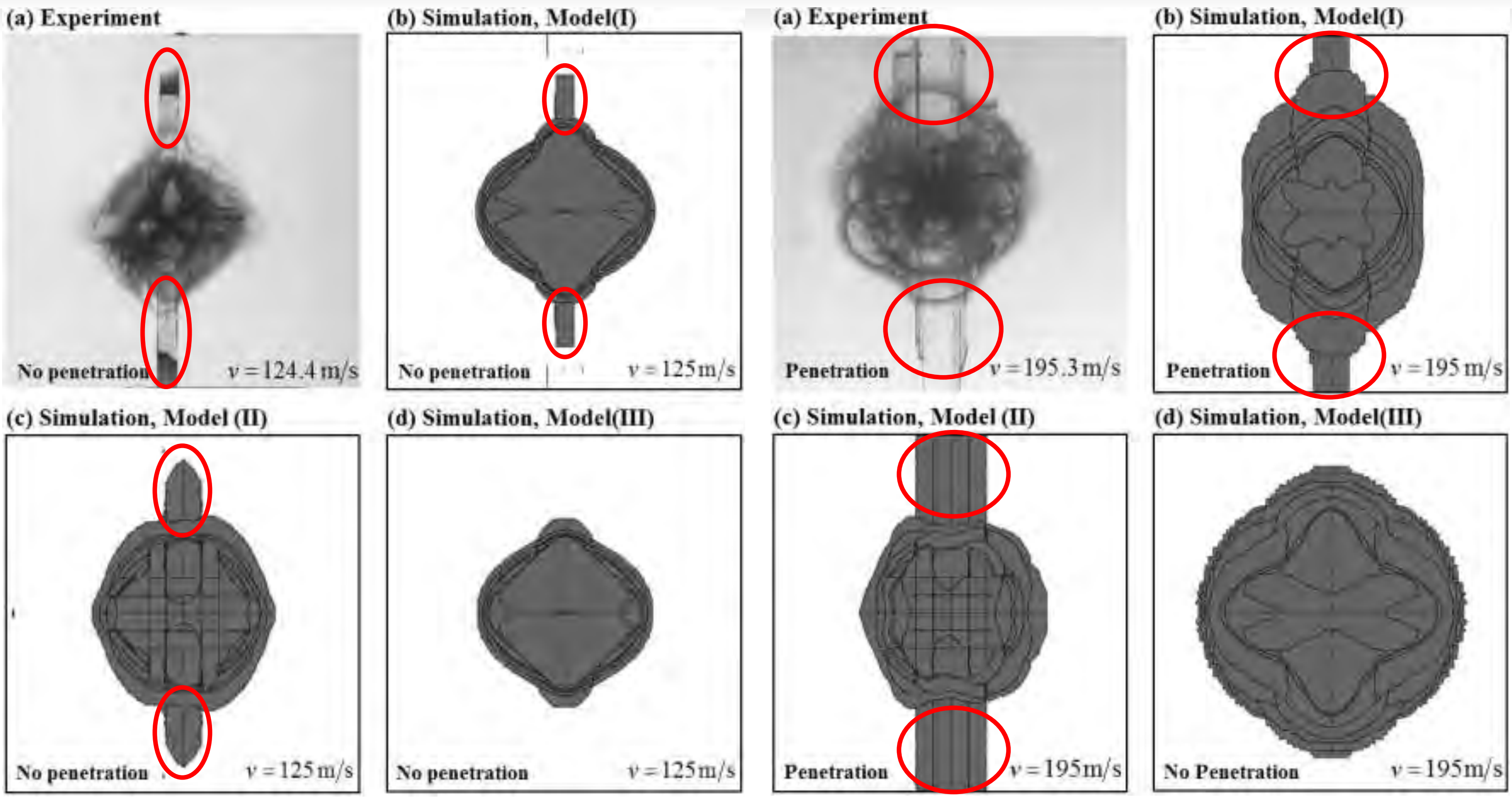


No penetration case

Penetration case

**Model (i) and (ii) can capture the large matrix cracks, but Model (iii) (i.e. CM) cannot address those cracks.**

# Results of damage areas and computational cost

Damage areas and Computation cost

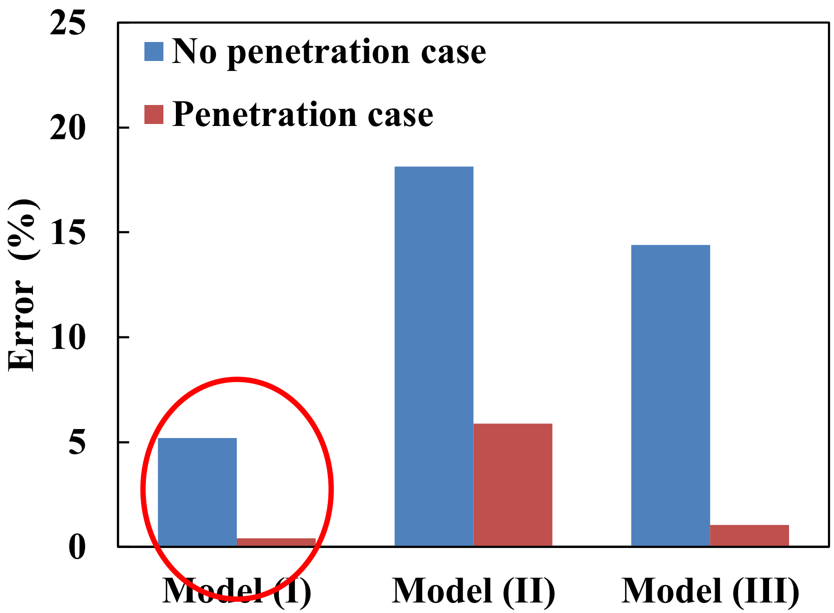


(i) Comparison of error of predicted damage area

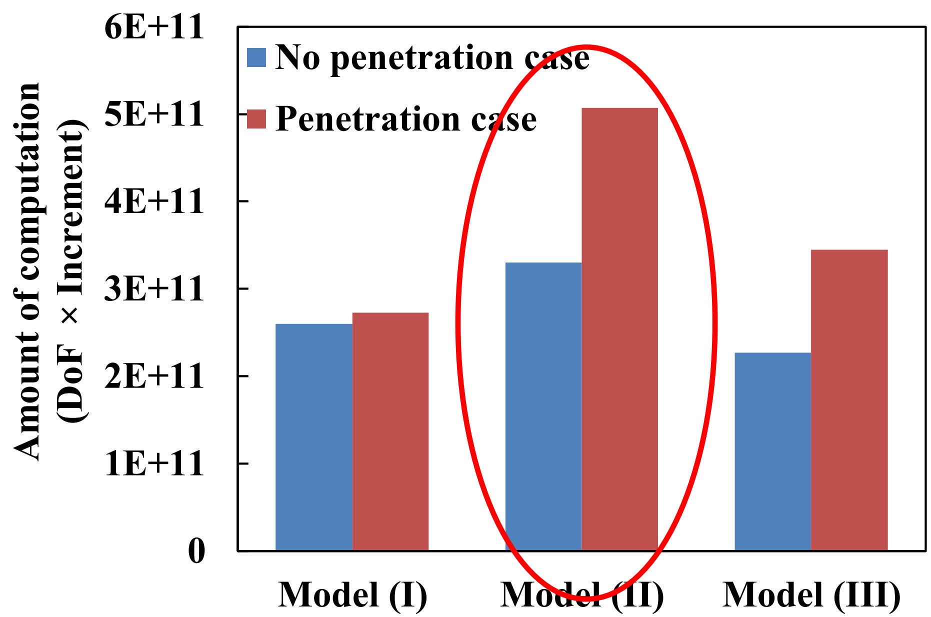


(ii) Comparison of amount of computation (DoF × Increment)

Highest-accuracy of prediction in damage area was given by Hybrid simulation model (Model (i)).

Model (ii) requires highest amount of computation, as like OHT.

# Analytical derivation of damage tensor for multiple cracks

Until now, I have explained the numerical modeling based on the damage mechanics using the following compliance matrix.

$$\begin{bmatrix} \varepsilon_z^p \\ \varepsilon_y^p \\ 2\varepsilon_{zy}^p \end{bmatrix} = \begin{bmatrix} \dfrac{1}{E_1} & -\dfrac{\nu_{12}}{(1-d_2)E_1} & 0 \\ -\dfrac{\nu_{12}}{E_1} & \dfrac{1}{(1-d_2)E_2} & 0 \\ 0 & 0 & \dfrac{1}{2G_{12}}\left(1+\dfrac{1}{1-d_2}\right) \end{bmatrix} \begin{bmatrix} \sigma_z^a \\ \sigma_y^a \\ \sigma_{zy}^a \end{bmatrix}$$

Damage tensor $d_2$ is generally used for expressing the stiffness reduction due to the multiple cracks, but the relationship between $d_2$ and crack density is still unclear!!
=>Here, we try to derive $d_2$ as a function of crack density $\rho$.

# Analytical derivation of damage tensor for multiple cracks

In this study, $d_2$ is formulated as a function of crack density using two-dimensional elasticity.

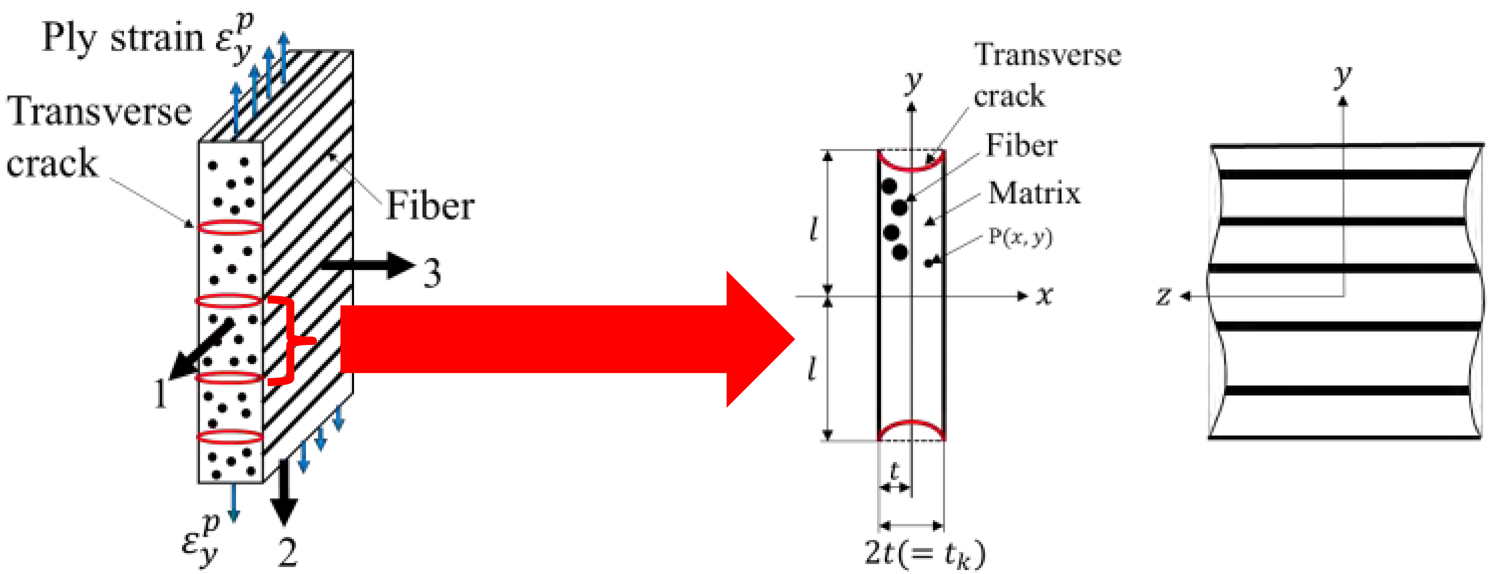


Corresponding ply including transverse crack

Representative 2D volume element

- The transverse crack is assumed to have a tunnel-like crack (which is symmetrical about the $y$ axis).

# Analytical derivation of damage tensor for multiple cracks

- The $y$ direction of displacement $v(x,y)$

$$v(x,y)=\frac{8l\varepsilon_y^p}{\pi^2}\sum_{n=1}^{\infty}\frac{(-1)^{n+1}}{(2n-1)^2}\frac{\cosh\left(\frac{2n-1}{2l}\pi\lambda x\right)}{\cosh\left(\frac{2n-1}{2l}\pi\lambda t\right)}\sin\left(\frac{2n-1}{2l}\pi y\right)$$

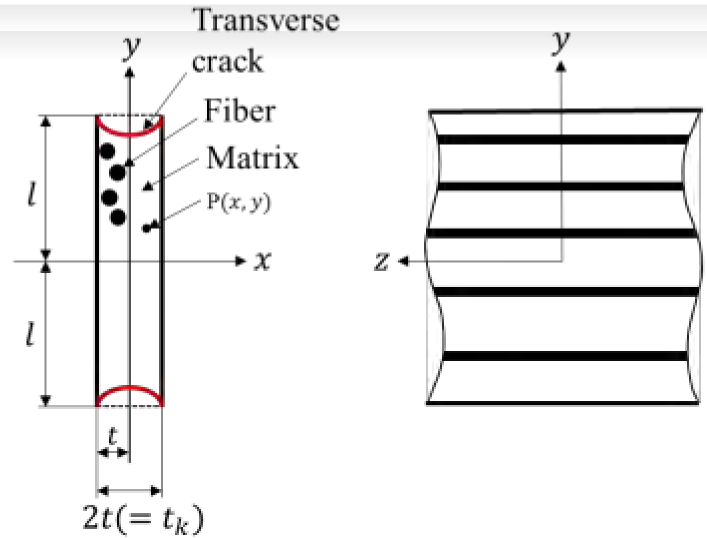


- The stresses $\sigma_x$ ,$\sigma_y$, and $\sigma_{xy}$ can be rewritten as

$$\sigma_x(x,y)=\frac{aC_1+C_2}{C_1^{\;2}-C_2^{\;2}}\frac{\partial v}{\partial y}=\frac{aC_1+C_2}{C_1^{\;2}-C_2^{\;2}}\left(\frac{4}{\pi}\sum_{n=1}^{\infty}\frac{(-1)^{n+1}}{2n-1}\frac{\cosh\left(\frac{2n-1}{2l}\pi\lambda x\right)}{\cosh\left(\frac{2n-1}{2l}\pi\lambda t\right)}\cos\left(\frac{2n-1}{2l}\pi y\right)\right)\varepsilon_y^p$$

$$\sigma_y(x,y)=\frac{C_1+aC_2}{C_1^{\;2}-C_2^{\;2}}\frac{\partial v}{\partial y}=\frac{C_1+aC_2}{C_1^{\;2}-C_2^{\;2}}\left(\frac{4}{\pi}\sum_{n=1}^{\infty}\frac{(-1)^{n+1}}{2n-1}\frac{\cosh\left(\frac{2n-1}{2l}\pi\lambda x\right)}{\cosh\left(\frac{2n-1}{2l}\pi\lambda t\right)}\cos\left(\frac{2n-1}{2l}\pi y\right)\right)\varepsilon_y^p$$

$$\sigma_{xy}(x,y)=G_{23}\frac{\partial v}{\partial x}=G_{23}\left(\frac{4\lambda}{\pi}\sum_{n=1}^{\infty}\frac{(-1)^{n+1}}{2n-1}\frac{\sinh\left(\frac{2n-1}{2l}\pi\lambda x\right)}{\cosh\left(\frac{2n-1}{2l}\pi\lambda t\right)}\sin\left(\frac{2n-1}{2l}\pi y\right)\right)\varepsilon_y^p$$

# Analytical derivation of damage tensor for multiple cracks

- The average ply strain $\varepsilon_y^a$ is given by

$$\varepsilon_y^a = \frac{1}{lt}\int_0^t v(x,l)dx$$

- The $y$ direction of displacement $v(x,y)$

$$v(x,y) = \frac{8l\varepsilon_y^p}{\pi^2}\sum_{n=1}^{\infty}\frac{(-1)^{n+1}}{(2n-1)^2}\frac{\cosh\left(\frac{2n-1}{2l}\pi\lambda x\right)}{\cosh\left(\frac{2n-1}{2l}\pi\lambda t\right)}\sin\left(\frac{2n-1}{2l}\pi y\right)$$

- Transverse crack density $\rho = 1/(2l)$

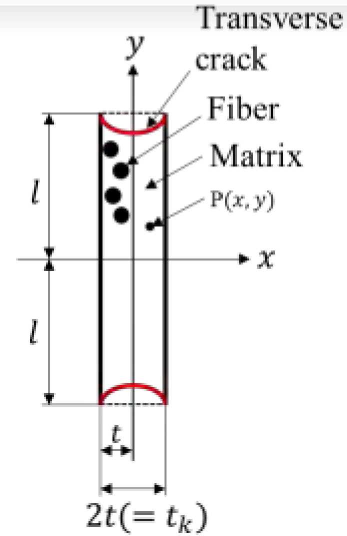


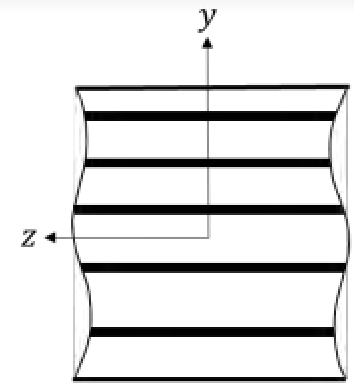


$$\frac{\varepsilon_y^a}{\varepsilon_y^p} = \sum_{n=1}^{\infty}\frac{16}{(2n-1)^3\pi^3\lambda t_k}\frac{\tanh\left[\frac{2n-1}{2}\pi\lambda t_k\rho\right]}{\rho}$$

$$d_2 = 1 - \sum_{n=1}^{\infty}\frac{16}{(2n-1)^3\pi^3\lambda t_k}\frac{\tanh\left[\frac{2n-1}{2}\pi\lambda t_k\rho\right]}{\rho}$$

Relationship between damage tensor and crack density

This is the main result of this study!!

TOHOKU

# Analytical derivation of damage tensor for multiple cracks

## Damage mechanics model of laminates

The effective compliance of laminate $\overline{\boldsymbol{C}}$ is formulated by classical laminate theory.

$$\overline{\boldsymbol{C}} = \left( \frac{1}{t_L} \sum_{k=1}^{N} t_k \left( \boldsymbol{R}_k \boldsymbol{C} \boldsymbol{T}_k^{-1} \right)^{-1} \right)^{-1}$$

$t_k$:Thickness of the laminate
$t_L$:Thickness of the $k$−th ply
$\boldsymbol{R}_k$: Coordinate conversion of the strain
$\boldsymbol{T}_k$: Coordinate conversion of the stress
$C$ : Effective compliance of the ply

## Damage mechanics model of the ply

The effective compliance of the ply $\boldsymbol{C}$ is described by using a continuum damage mechanics (CDM) model.

$$\boldsymbol{C} = \boldsymbol{C}_0 \boldsymbol{M}$$

$$\boldsymbol{M} = \begin{bmatrix} 1 & 0 & 0 \\ 0 & \frac{1}{1-d_2} & 0 \\ 0 & 0 & \frac{1}{2}\left(1 + \frac{1}{1-d_2}\right) \end{bmatrix}$$

$\boldsymbol{M}$: Damage effective tensor
$\boldsymbol{C}_0$: Compliance of the ply under undamaged conditions
$d_2$: Damage variable in the direction normal to the fiber
$\rho$: Transverse crack density

$$d_2 = 1 - \frac{16}{\pi^3 \lambda t_k} \sum_{n=1}^{\infty} \frac{1}{(2n-1)^3} \frac{\tanh\left[(2n-1)\pi\lambda t_k \rho/2\right]}{\rho}$$

We can determine the effective stiffness of the damaged composite laminate.

# Analytical derivation of damage tensor for multiple cracks

## Cross-ply laminate

Comparison with experimental results Groves et al. [6)]

- Material : CFRP
- Lay-up configuration : $[0/90]_s$, $[0_2/90_2]_s$

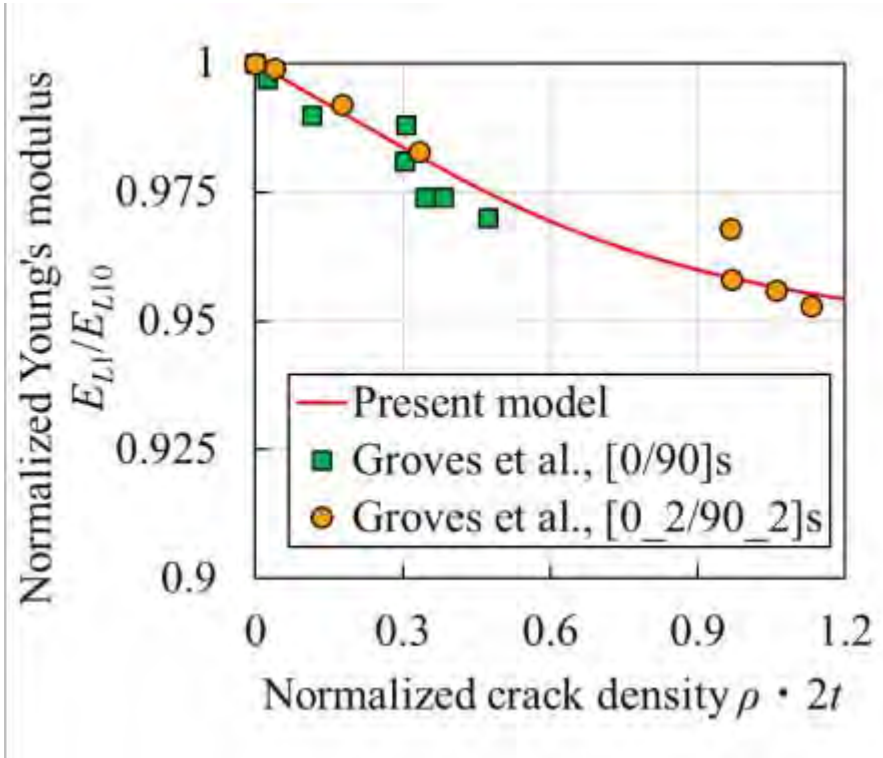


The result shows good agreement with the results obtained by Groves et al.


6) S. E. Groves, C. E. Harris, A. L. Highsmith, D. H. allen and R. G. Norvell : *Expl Mech.* , **27,** 1 (1987), 73-79.

# Analytical derivation of damage tensor for multiple cracks

## Angle-ply laminate

7) P. Gudmundson and W. Zang *Int. J. Solids Structures*, **30**(1993)23, pp. 3211-3231.

Comparison with FEA results obtained by Gudmundson et al.[7)]

- Material : GFRP
- Lay-up configuration : $[\pm 55]_N$, $[\pm 67.5]_N$

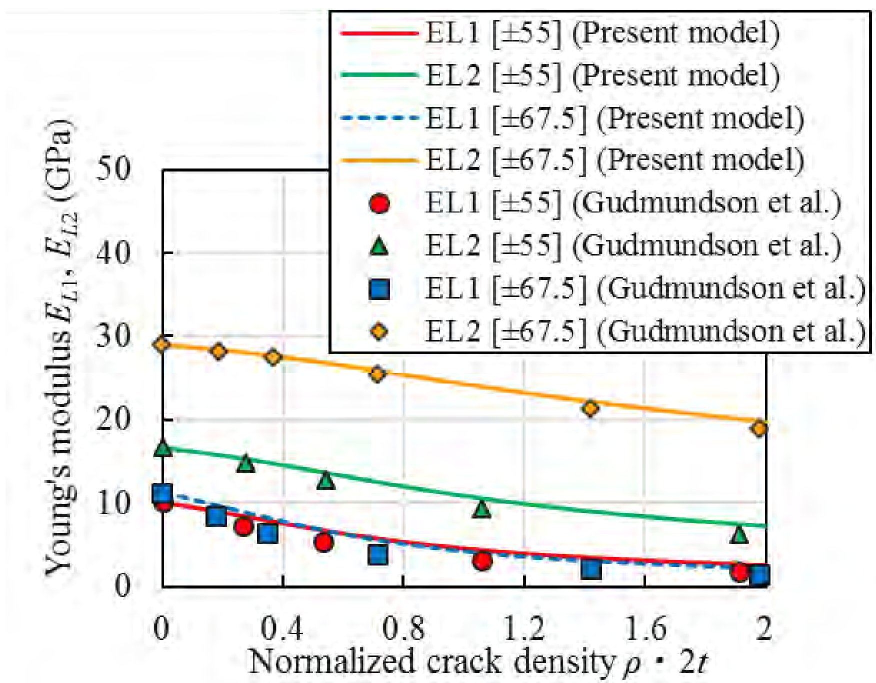


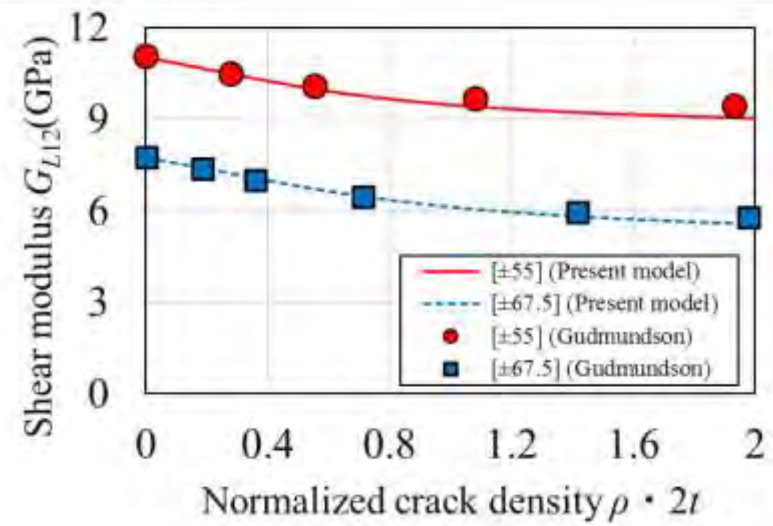


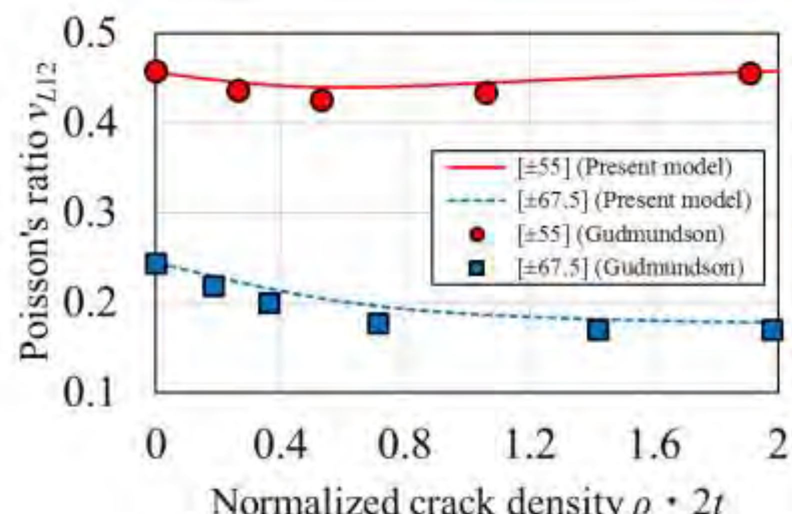


All of properties agreed well with the calculated results by Gudmundson et al.

# Analytical derivation of damage tensor for multiple cracks

## Quasi-isotropic laminate

Comparison with experimental results obtained by Tong et al. [8)]

- Material : GFRP
- Lay-up configuration : $[0/90/-45/+45]_s$
- The calculation is conducted assuming approximately the same damage occurrence due to transverse cracking in the 90° and ±45° plies.

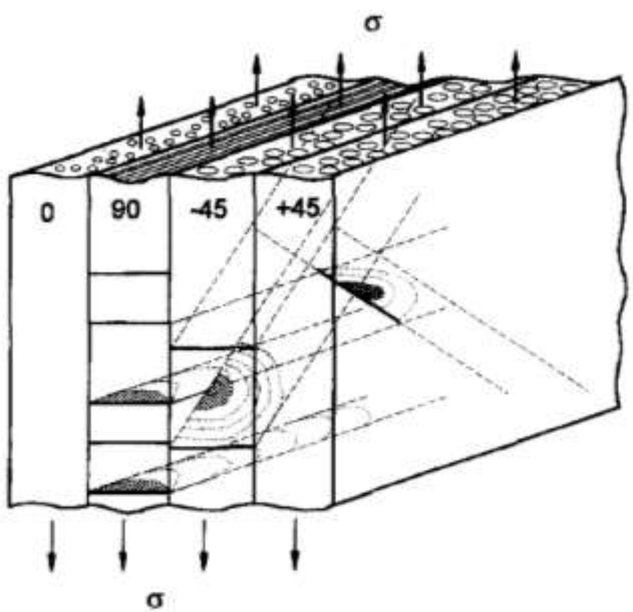


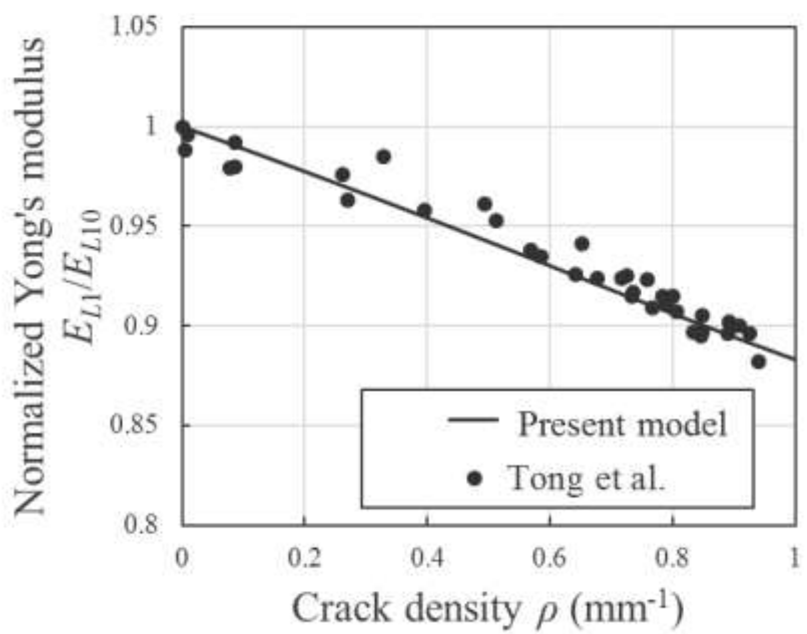


The result shows good agreement with the results obtained by Tong et al.

8) J. Tong, F. J. Guild, S. L. Ogin and P. A. Smith : *Comp. Sci. Tech.* , **57,** (1997), pp. 1527-1535.

# Summary of Analytical derivation of damage tensor for multiple cracks

In this study, the local stress distribution in a ply including transverse cracks was formulated, and the stiffness reduction of laminate was investigated using the local displacement distribution. We also derived the relationship between damage tensor and crack density analytically.

✓ If you use this relationship obtained from the analytical derivation, you can convert the damage tensor into the crack densities as shown in the figure.

$$d_2 = 1 - \frac{16}{\pi^3 \lambda t_k} \sum_{n=1}^{\infty} \frac{1}{(2n-1)^3} \frac{\tanh\left[(2n-1)\pi\lambda t_k \rho/2\right]}{\rho}$$

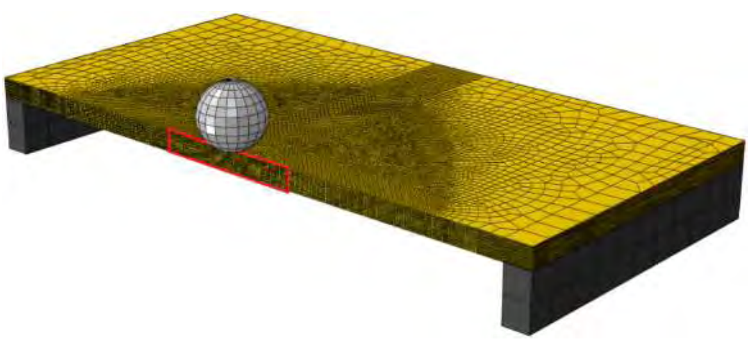

8) J. Tong, F. J. Guild, S. L. Ogin and P. A. Smith : *Comp. Sci. Tech.* , **57,** (1997), pp. 1527-1535.

- 切削モデル[1]　:ドリルを円錐形の圧子に置き換える
  :圧子に接する要素を逐次削除することで切削現象を解析

材料と接触する際に生じる圧子表面の圧力から要素削除判定

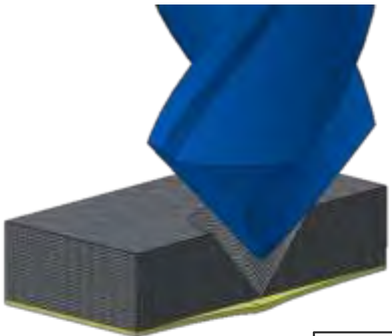

従来のドリルモデル
- ドリル形状をモデル化
- 回転の影響を考慮可
- 解析コスト大

押し込みによるはく離のみに注目

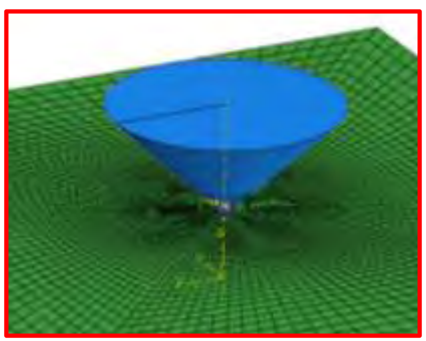

本解析でのモデル
- ドリルを円錐形に置換
- 回転の影響は考慮しない
- 解析コスト小

ドリル形状の単純化

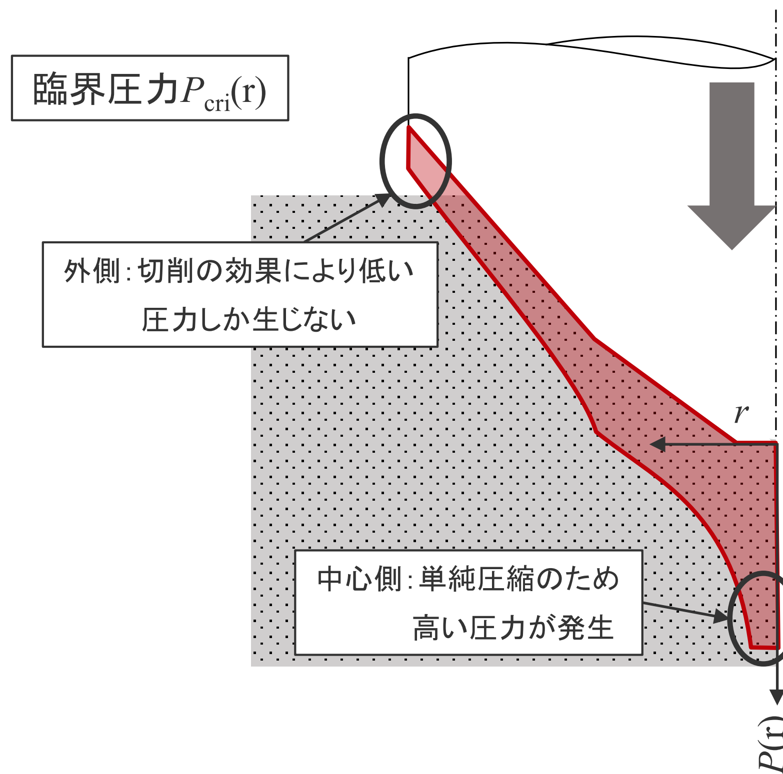


要素削除の概要

[1]Park Sang Chul,東京大学博士論文,2013

# Numerical Modeling for Drilling Damage

- 切削モデル[1]　:ドリルを円錐形の圧子に置き換える
  :圧子に接する要素を逐次削除することで切削現象を解析

材料と接触する際に生じる圧子表面の圧力から要素削除判定

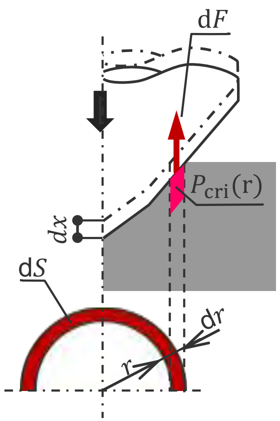


$$dF = P_{cri}(\mathrm{r})dS \quad (1)$$

$$= P_{cri}(r)2\pi r dr \quad (2)$$

$$P_{cri}(r) \begin{cases} = \text{圧縮強度}X_c \quad (0 \le r <^{*} r_1) \\ = \dfrac{dF}{dr_1}\dfrac{1}{2\pi r} \quad (r_1 \le r < r_2) \\ = \dfrac{dF}{dr_2}\dfrac{1}{2\pi r} \quad (r_2 \le r) \end{cases} \quad (3)$$

*$r_1$はチゼルエッジ半径としている.

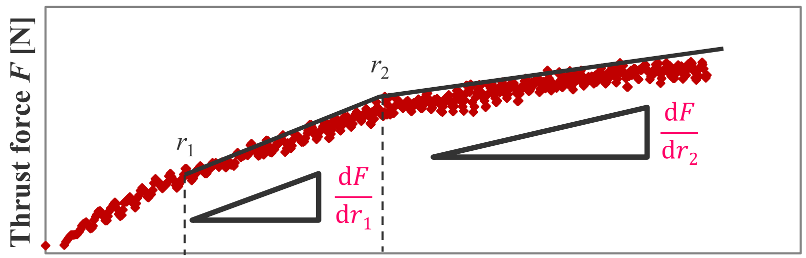


貫通実験から得られる勾配

臨界圧力$P_{cri}(r)$の決定方法

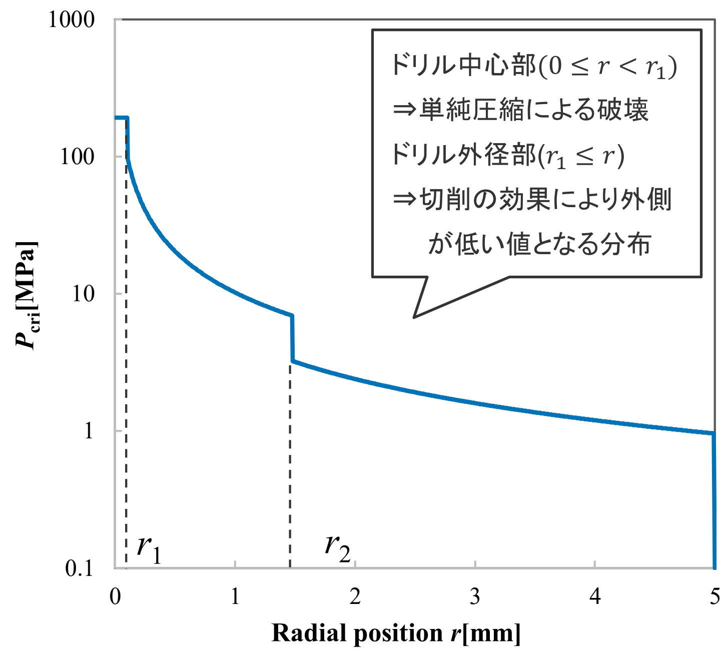


$f$ = 375 mm/min時の臨界圧力(Eq.(3))

臨界圧力の計算結果


[1]Park Sang Chul,東京大学博士論文,2013

# Numerical Modeling for Drilling Damage

- ソフトウェア　:Abaqus/Explicit(動的陽解法)
- 損傷モデル　:マトリクス破壊をCDM，繊維破壊をSCM，層間はく離をCZMで実装
  :CZMは第15-16層間，第16層トランスバースクラック部，GFRPに挿入
- 切削モデル　:切削現象を単純圧縮に置き換え⇒ドリルを圧子に置き換え
  :V-UMATにより実装した臨界圧力で切削現象を解析

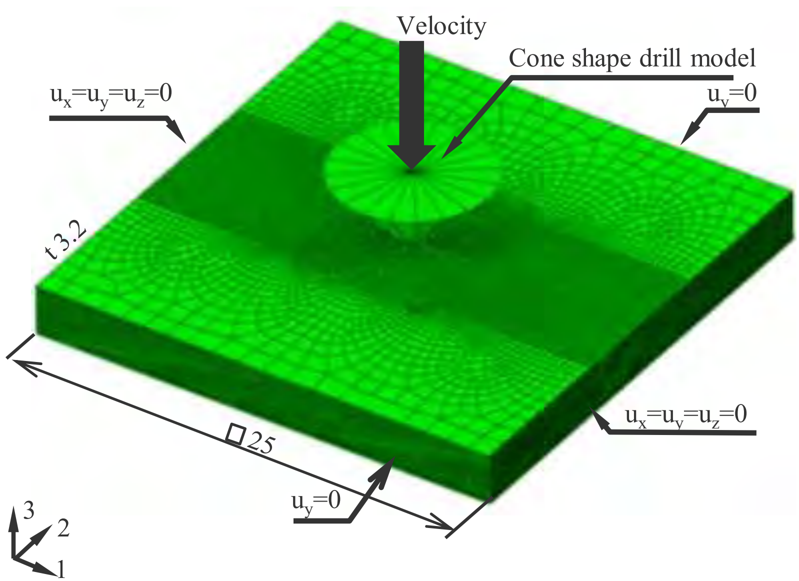

解析モデルと境界条件

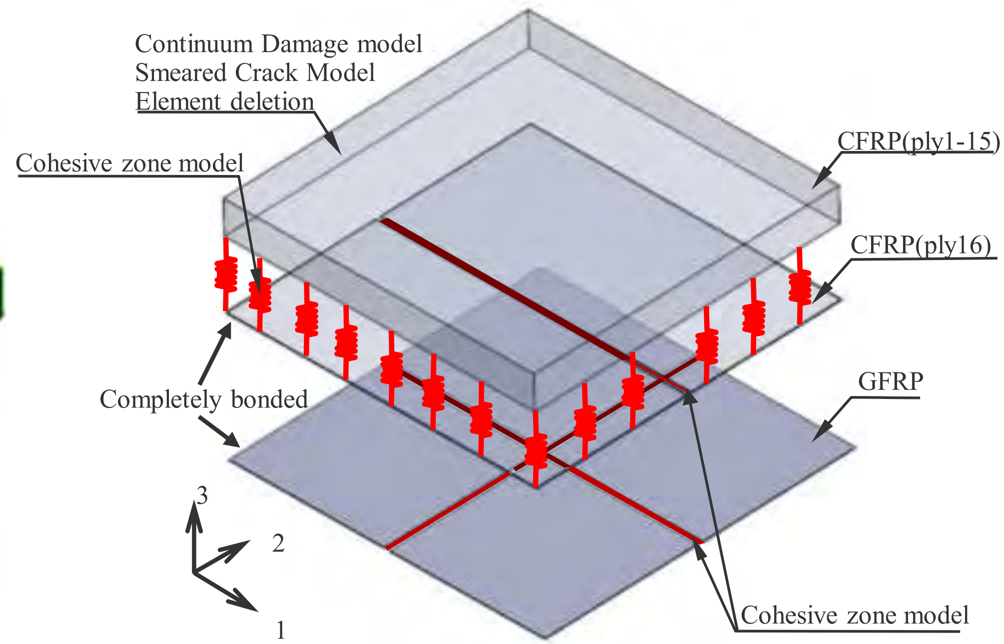

実装されている損傷モデルと材料

# Numerical Modeling for Drilling Damage

- ソフトウェア　：Abaqus/Explicit(動的陽解法)
- 損傷モデル　：マトリクス破壊をCDM，繊維破壊をSCM，層間はく離をCZMで実装
  ：CZMは第15-16層間，第16層トランスバースクラック部，GFRPに挿入
- 切削モデル　：切削現象を単純圧縮に置き換え⇒ドリルを圧子に置き換え
  ：V-UMATにより実装した臨界圧力で切削現象を解析

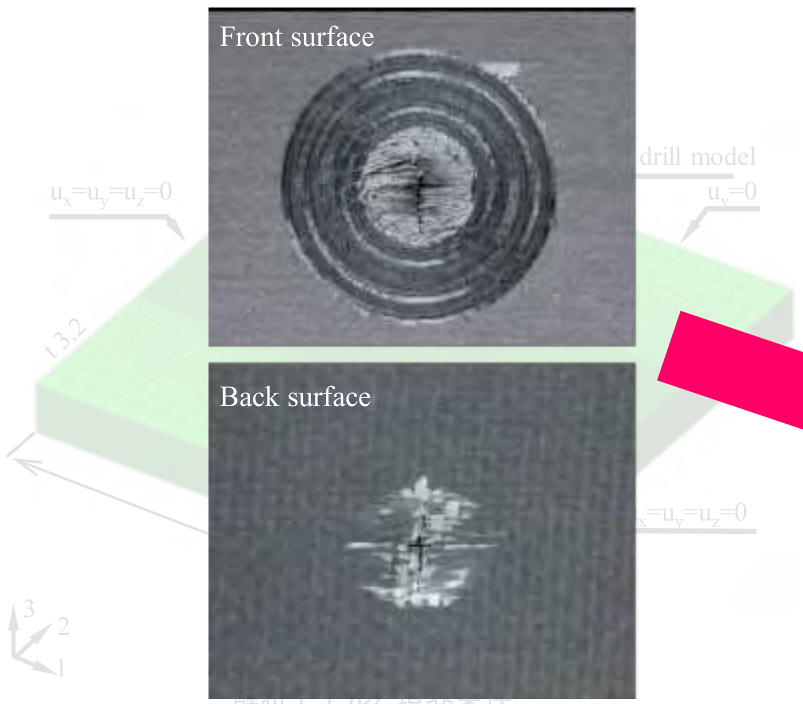


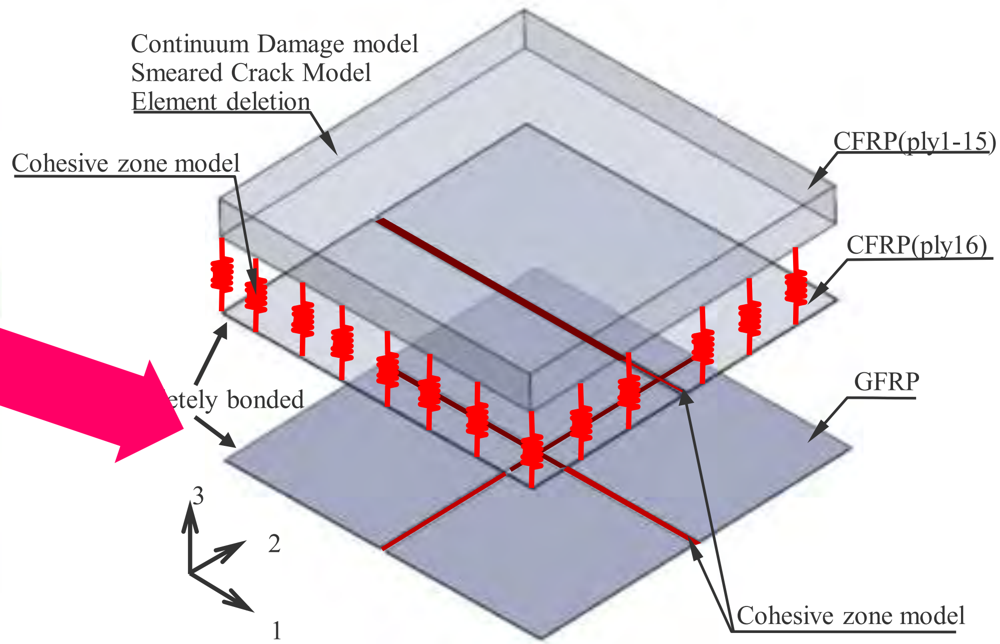


実装されている損傷モデルと材料

# Numerical Modeling for Drilling Damage

・結果

十字クラックを実装した損傷解析により，実験と同規模の損傷が生じた

⇒スラスト荷重の振動に起因し，**実験より早いタイミングで損傷が発生**

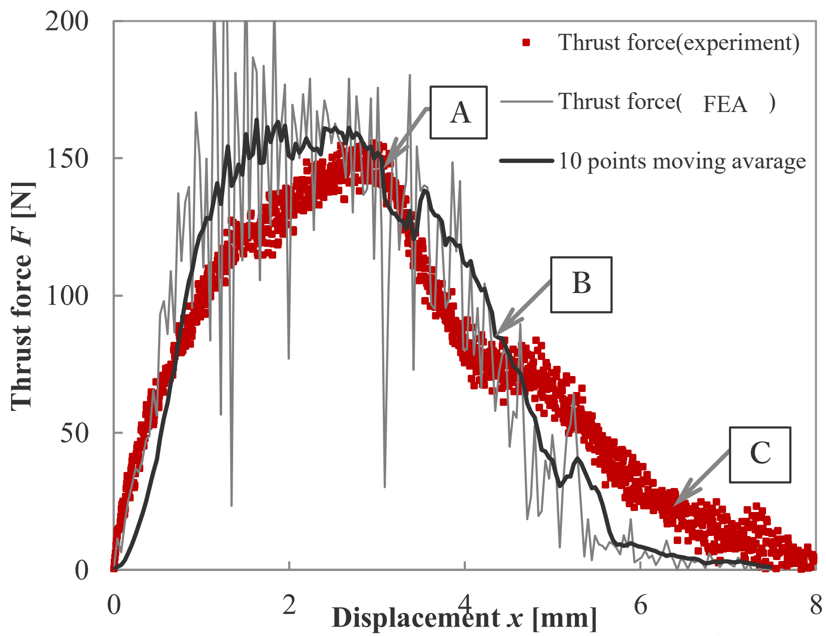

数値解析から得られたスラスト履歴と実験値の比較

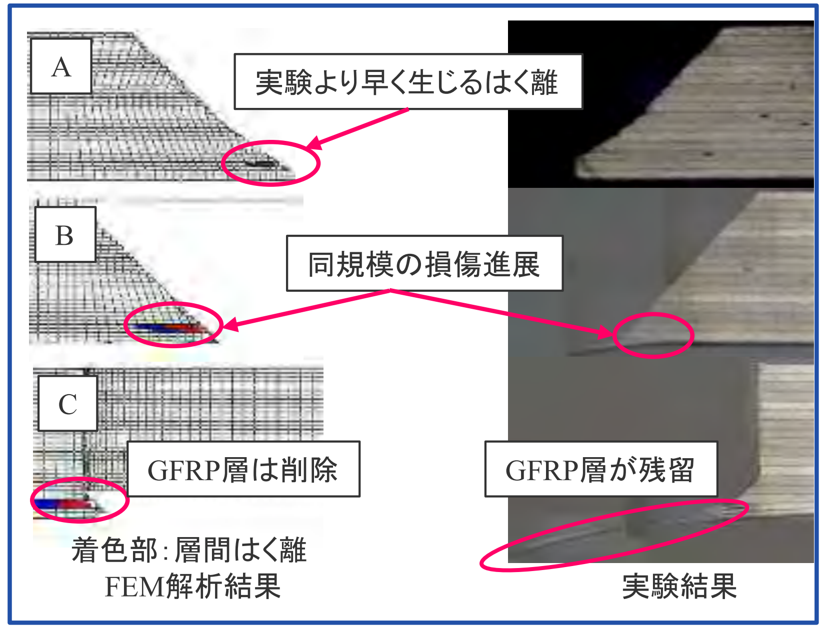

数値解析から得られた層間はく離と実験結果の比較

・結論

CFRP第16層トランスバースクラックおよびGFRPの十字クラック実装⇒損傷過程が再現

⇒層間はく離挙動は**背面に貼る材料の破壊挙動**に支配されていることが判った．

# Analytical Modeling for Drilling Damage

・理論解に用いる基礎式[6]

エネルギーのつり合い式　$\mathrm{d}W = \mathrm{d}U + \mathrm{d}G$ (1)

⇒dW ： ドリルの押し込み仕事dW

dU ： 円板のひずみエネルギdU

dG ： はく離時の損傷エネルギdG

$$\mathrm{d}W = \frac{F^2 a}{8\pi M}\mathrm{d}a \ (2) \quad \mathrm{d}U = \frac{1}{16}\frac{F^2 a}{\pi M}\mathrm{d}a \ (3) \quad \mathrm{d}G = G_{IC} \times 2\pi a \mathrm{d}a \ (4)$$

*Timoshenkoの円板曲げ理論より曲げ剛性　$M = \frac{Eh^2}{12(1-\nu^2)}$ (5)

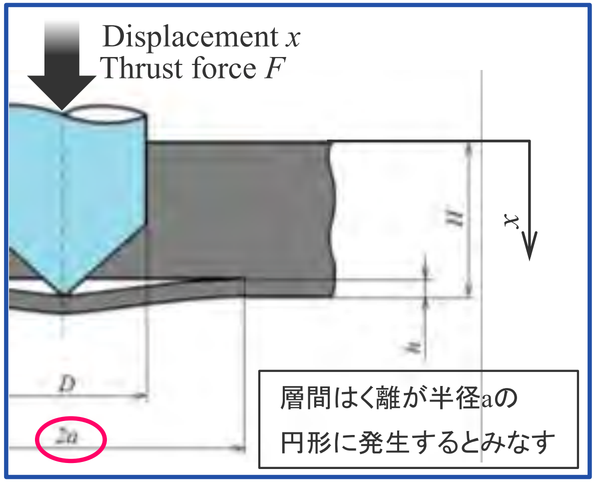


ドリル先端での円板対称曲げモデル

・層間はく離が進展する条件を満たす臨界荷重$F_{cri}$

$$F_{cri} = \pi\sqrt{\frac{8G_{IC}Eh^3}{3(1-\nu^2)}} = \pi\sqrt{\frac{8G_{IC}E(H-x)^3}{3(1-\nu^2)}} \quad (6)$$

⇒ドリル先端が第16層に到達するタイミングで

層間はく離が進展する条件が満たされる.

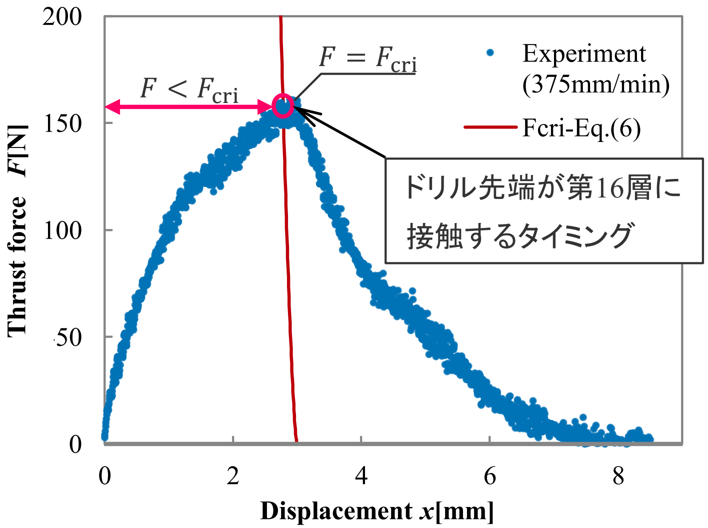


実験結果と荷重$F_{cri}$の比較

[6]H.Hocheng et al,*Journal of Materials Processing Technology*,2005

# Analytical Modeling for Drilling Damage

・理論解に用いる基礎式[4]

エネルギーのつり合い式　$dW = dU + dG$ (1)

⇒dW ： ドリルの押し込み仕事dW

$dU$ ： 円板のひずみエネルギ$dU$

$dG$ ： はく離時の損傷エネルギ$dG$

$dW = \frac{F^2}{8\pi \cdots}$

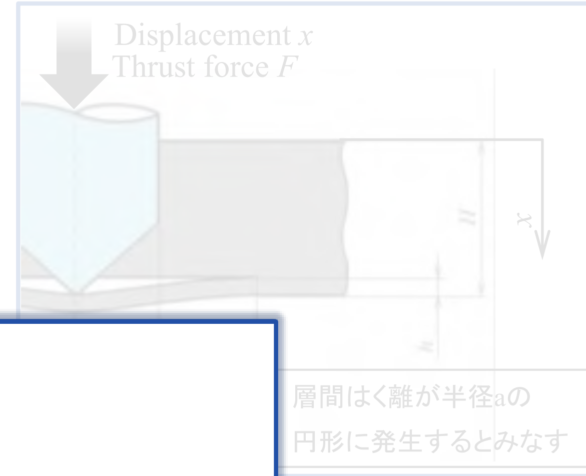

円板対称曲げモデル

理論解を用いた層間はく離発生条件の検討

・結論

ドリル先端が貫通する間際まで層間はく離は進展しない.

GFRP層の損傷に伴って層間はく離が発生する.

・層間はく離が

$$F_{cri} = \pi\sqrt{\frac{8G_{IC}Eh^3}{3(1-\nu^2)}} = \pi\sqrt{\frac{8G_{IC}E(H-x)^3}{3(1-\nu^2)}} \quad (6)$$

⇒ドリル先端が第16層に到達するタイミングで

層間はく離が進展する条件が満たされる.

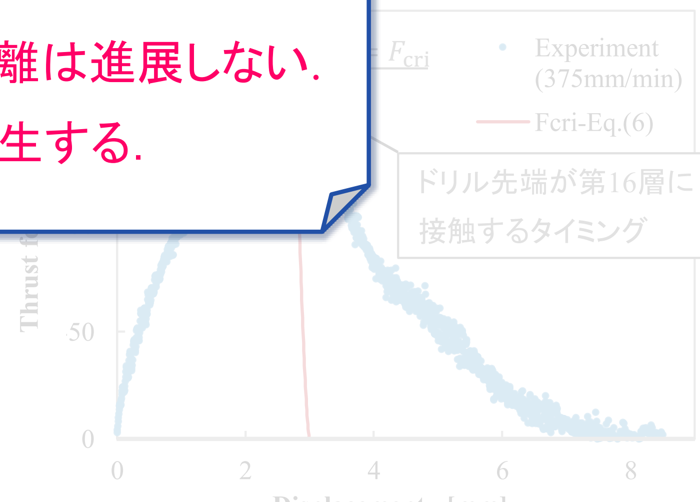

実験結果と荷重$F_{cri}$の比較

東北大学

# Analytical Modeling for Drilling Damage

・得られた積層板スケールでの損傷プロセス

StepI :ドリルがGFRP+16層に接触し，トランスバースクラック・層間はく離が発生

StepII :ドリル押し込みに伴い，背面のクラックに連動し層間はく離が進展

StepIII:GFRP+16層が強い曲げ・切削により削除され，損傷が収束

⇒穿孔加工下での層間はく離は，背面に貼る材料の損傷挙動に支配されている

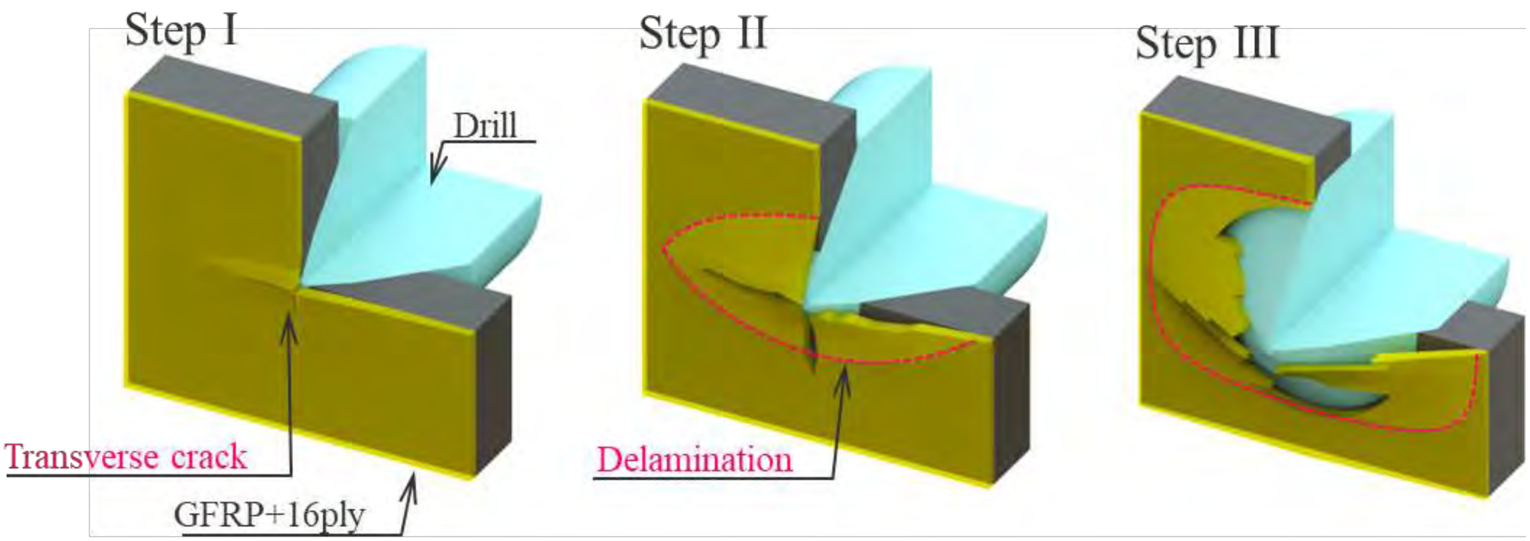

# 検証　様々な加工条件に対する解析モデルの適用

・加工中に送り速度を変化させる加工

⇒加工時間を短縮しつつ穿孔損傷を最小限にする

⇒構築した数値解析モデルにより3パターンの加工条件を解析，実験と比較

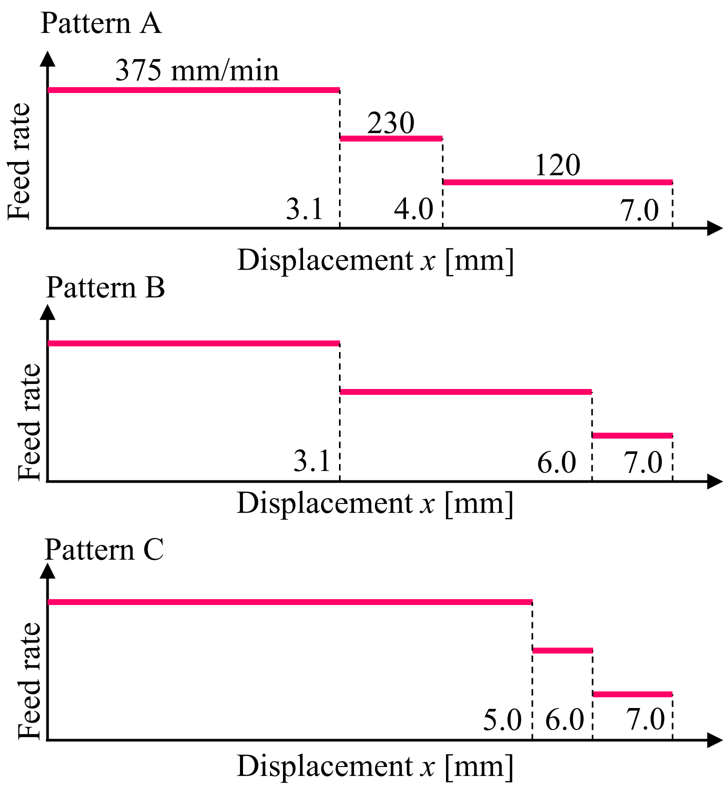


各加工条件におけるドリル先端の臨界圧力

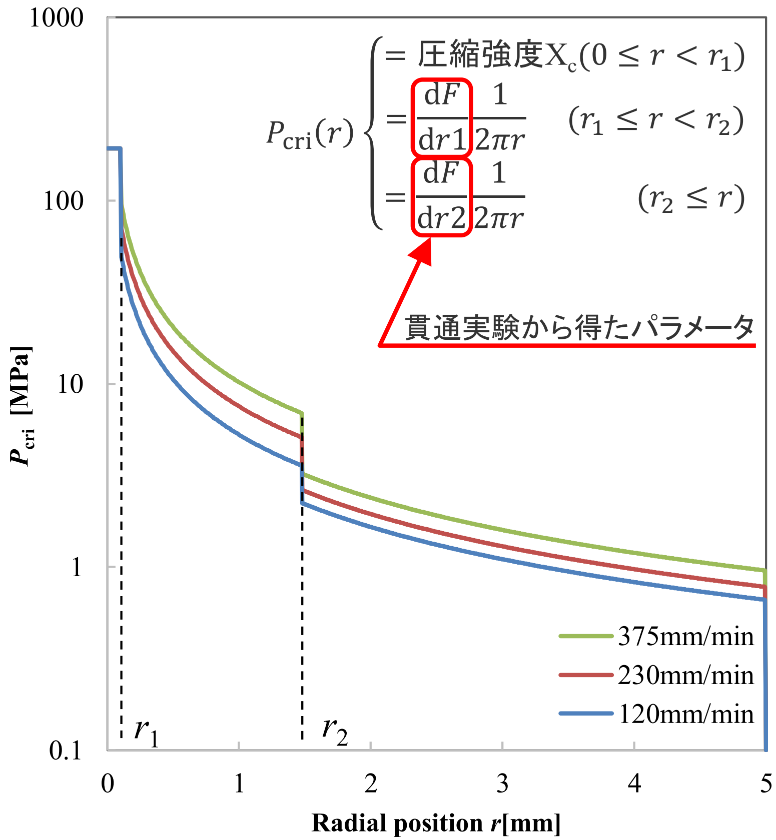

# 検証　様々な加工条件に対する解析モデルの適用

- 加工中に送り速度を変化させる加工
  - ⇒損傷の形状は実験結果を良く再現した．
  - ⇒数値解析では残留した最終層が早期削除されるため，損傷を過小評価した．

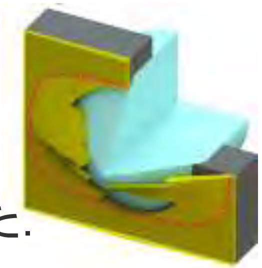

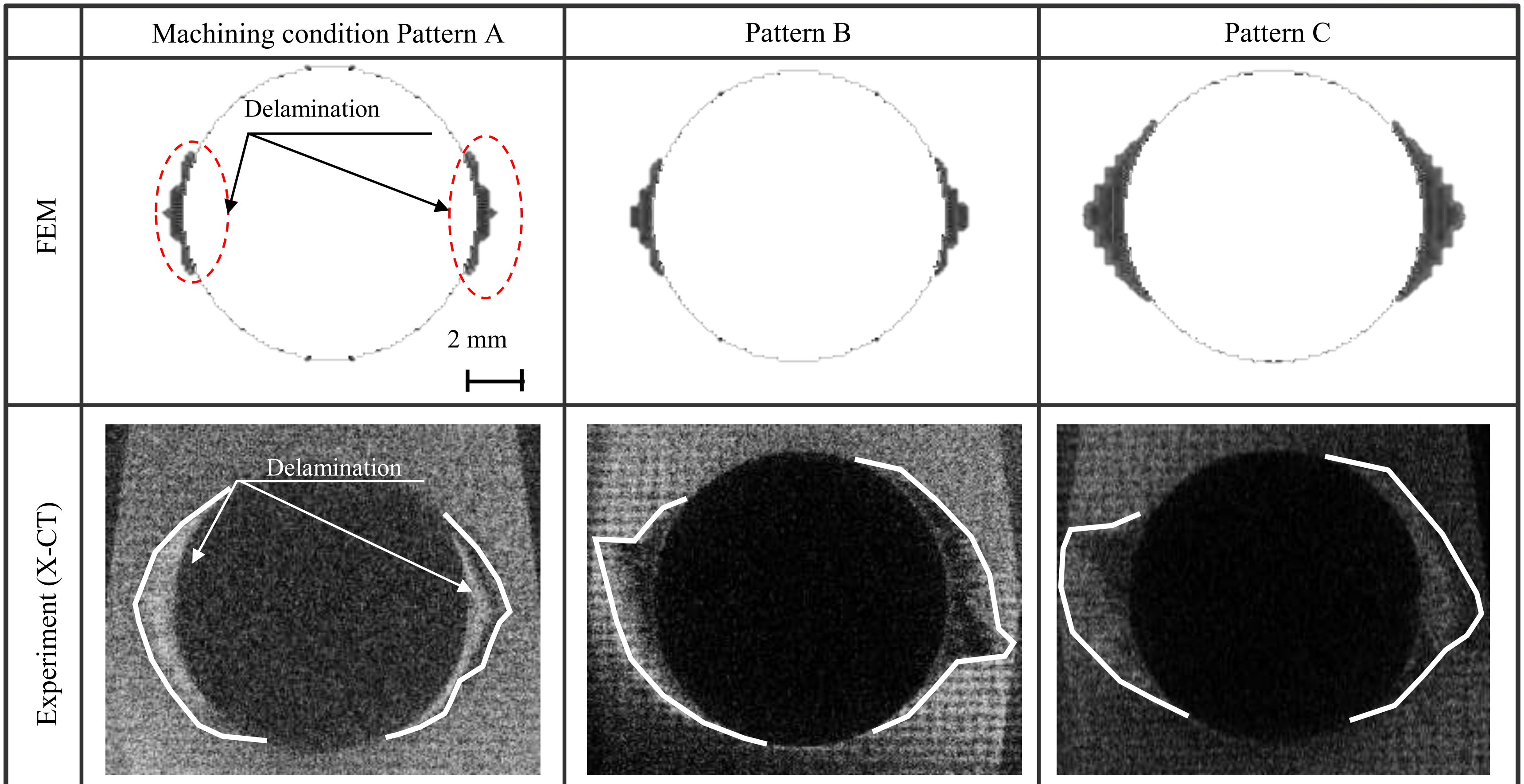

# 検証　様々な加工条件に対する解析モデルの適用

- 加工中に送り速度を変化させる加工

  ⇒損傷の形状は実験結果を良く再現した.

  ⇒数値解析では残留した最終層が早期削除されるため，損傷を過小評価した.

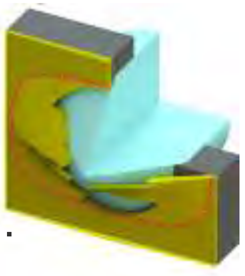

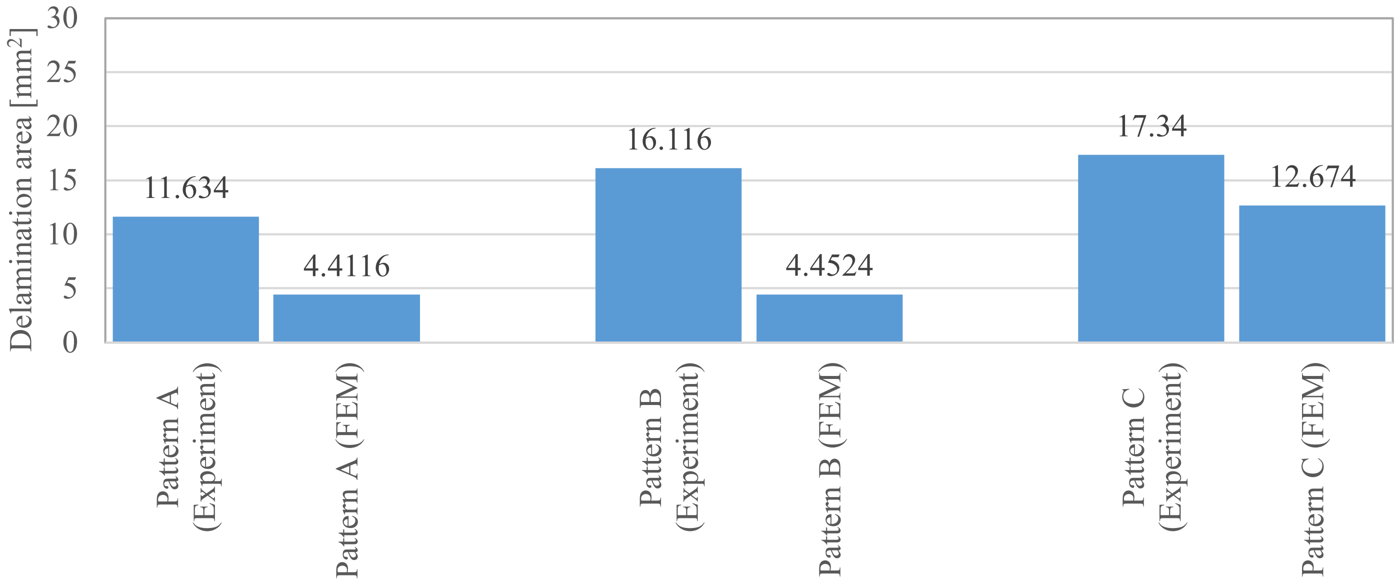


- 結論

  本研究で構築した解析モデルにより，各加工条件での損傷傾向が定性的に再現された.

  ⇒加工条件を変えた場合でも，層間はく離挙動は最終層の損傷挙動に支配される.

  ⇒損傷面積を評価するためには，最終層の要素削除基準の改善が必要.

# Conclusions

・実験・FEM・理論解から得られた結論

実験　:GFRP+第16層の一部が残留+押出を受けて損傷が進展する

FEM　:層間はく離挙動は第16層トランスバースクラック,GFRPの十字クラックに支配

理論解 :ドリル先端が貫通する間隙まで層間はく離は進展しない

・得られた積層板スケールでの損傷プロセス

StepI :ドリルがGFRP+16層に接触し，トランスバースクラック・層間はく離が発生

StepII :ドリル押し込みに伴い，背面のクラックに連動し層間はく離が進展

StepIII:GFRP+16層が強い曲げ・切削により削除され，損傷が収束

⇒穿孔加工下での層間はく離は，背面に貼る材料の損傷挙動に支配されている

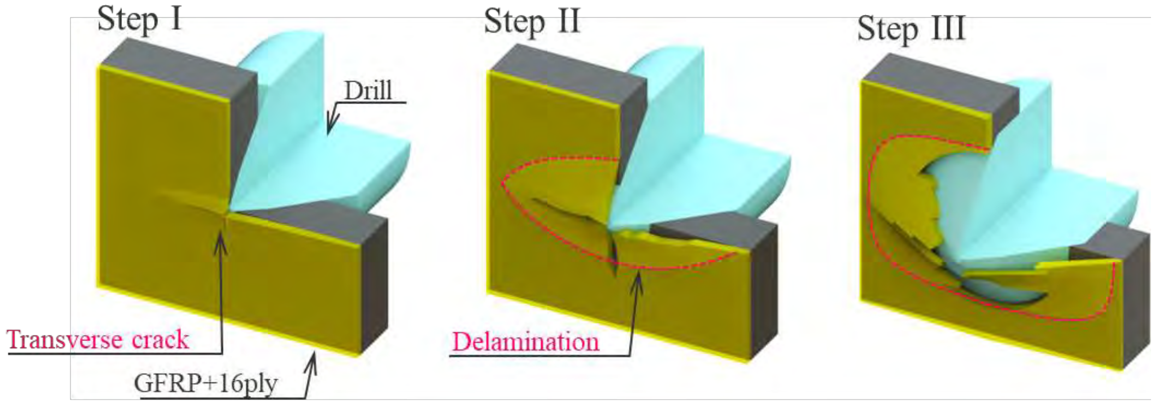


研究成果の活用例

・構造体破壊解析への穿孔損傷実装

⇒損傷プロセスを踏まえた形状・位置決定

・FEM解析を用いた背面の破壊予測

⇒背面パッチに適した物性の同定

⇒既存ドリルの限界加工条件決定